Renal Denervation Suppresses Coronary Hyperconstricting Responses After Drug-Eluting Stent Implantation in Pigs in Vivo Through the Kidney–Brain–Heart Axis

Hironori Uzuka, Yasuharu Matsumoto, Kensuke Nishimiya, Kazuma Ohyama, Hideaki Suzuki, Hirokazu Amamizu, Susumu Morosawa, Michinori Hirano, Tomohiko Shindo, Yoku Kikuchi, Kiyotaka Hao, Takashi Shiroto, Kenta Ito, Jun Takahashi, Koji Fukuda, Satoshi Miyata, Yoshihito Funaki, Hatsue Ishibashi-Ueda, Satoshi Yasuda, Hiroaki Shimokawa

Objective—Drug-eluting stent–induced coronary hyperconstricting responses remain an important issue. The adventitia harbors a variety of components that potently modulate vascular tone, including sympathetic nerve fibers (SNF) and vasa vasorum. Catheter-based renal denervation (RDN) inhibits sympathetic nerve activity. We, thus, examined whether RDN suppresses drug-eluting stent–induced coronary hyperconstricting responses, and if so, what mechanisms are involved.

Approach and Results—Protocol 1: pigs implanted with everolimus-eluting stents into the left coronary arteries underwent coronary angiography at 1 month after implantation for assessment of coronary vasomotion and adventitial SNF formation. Drug-eluting stent–induced coronary hyperconstricting responses were significantly enhanced associated with enhanced coronary adventitial SNF and vasa vasorum formation.Protocol 2: pigs implanted with everolimus-eluting stents were randomly assigned to the RDN or sham group. The RDN group underwent renal ablation. At 1 month, RDN significantly caused marked damage of the SNF at the renal arteries without any stenosis, thrombus, or dissections. Notably, RDN significantly upregulated the expression of α_2-adrenergic receptor–binding sites in the nucleus tractus solitarius, attenuated muscle sympathetic nerve activity, and decreased systolic blood pressure and plasma renin activity. In addition, RDN attenuated coronary hyperconstricting responses associated with decreases in SNF and vasa vasorum enhancements, inflammatory cell infiltration, and Rho-kinase expression/activation. Furthermore, there were significant positive correlations between SNF and vasa vasorum and between SNF and coronary vasoconstricting responses.

Conclusions—These results provide the first evidence that RDN ameliorates drug-eluting stent–induced coronary hyperconstricting responses in pigs in vivo through the kidney–brain–heart axis. (***Arterioscler Thromb Vasc Biol.* 2017;37:00-00. DOI: 10.1161/ATVBAHA.117.309777.**)

Key Words: blood pressure ■ coronary vessels ■ nerve fibers ■ renal artery ■ stents

Downloaded from http://atvb.ahajournals.org/ by guest on August 20, 2017

ATVB Arteriosclerosis, Thrombosis, and Vascular Biology FIRST PROOF ONLY

Although drug-eluting stents (DES) reduce the risk of restenosis and repeated revascularization after percutaneous coronary intervention, they occasionally cause unfavorable effects, such as stent thrombosis[1] and coronary hyperconstricting responses, not only to acetylcholine[2] but also to exercise.[3] We and others have recently demonstrated high prevalence of coronary vasomotor abnormalities after percutaneous coronary intervention (≈50%) in both white and Japanese patients.[4,5] Furthermore, recent clinical trial showed that new or worsening angina was also documented in 30% of patients who underwent successful percutaneous coronary intervention with the most promising DES, everolimus-eluting stents.[6] Thus, DES-induced coronary hyperconstricting responses are an emerging worldwide concern after stent implantation.[4–6]

We have previously demonstrated that activation of Rho-kinase pathway—a central mechanism of coronary spasm—in vascular smooth muscle cells plays key roles in the pathogenesis of coronary spasm[7,8] and DES-induced coronary hyperconstricting responses in animals[9] and humans.[2] Importantly, coronary adventitial inflammation, including infiltration of macrophages, and interleukin-1β–positive cells are involved in the pathogenesis of coronary spasm.[10–12] We also have demonstrated that formation of coronary adventitial vasa vasorum (VV), which are nutrient blood vessels of the vascular wall,

Received on: June 7, 2017; final version accepted on: August 2, 2017.

From the Department of Cardiovascular Medicine, Tohoku University Graduate School of Medicine, Sendai, Japan (H.U., Y.M., K.N., K.O., H. Suzuki, H.A., S.M., M.H., T.S., Y.K., K.H., T.S., K.I., J.T., K.F., S.M., H. Shimokawa); Wellman Center for Photomedicine, Massachusetts General Hospital, Boston (K.N.); Division of Brain Sciences, Department of Medicine, Imperial College London, United Kingdom (H. Suzuki); Cyclotron and Radioisotope Center, Tohoku University, Sendai, Japan (Y.F.); and Department of Pathology (H.I.-U.) and Department of Cardiovascular Medicine (S.Y.), National Cerebral and Cardiovascular Center, Suita, Japan.

This manuscript was sent to Philip Tsao, Consulting Editor, for review by expert referees, editorial decision, and final disposition.

The online-only Data Supplement is available with this article at http://atvb.ahajournals.org/lookup/suppl/doi:10.1161/ATVBAHA.117.309777/-/DC1.

Correspondence to Hiroaki Shimokawa, MD, PhD, Department of Cardiovascular Medicine, Tohoku University Graduate School of Medicine, 1-1 Seiryo-ma chi, Aoba-ku, Sendai 980-8574, Japan. E-mail shimo@cardio.med.tohoku.ac.jp

© 2017 American Heart Association, Inc.

Nonstandard Abbreviations and Acronyms

BP	blood pressure
DES	drug-eluting stent
NGF	nerve growth factor
NPY	neuropeptide Y
NTS	nucleus tractus solitarius
RDN	renal denervation
SNF	sympathetic nerve fiber
VV	vasa vasorum
TH	tyrosine hydroxylase

is enhanced in the coronary adventitia of patients with vasospastic angina.[13] We also have recently reported that enhanced VV formation in the coronary adventitia after DES implantation is closely associated with coronary hyperconstricting responses.[12]

The adventitia harbors a variety of components that potently modulate vascular tone, including not only inflammatory cells and VV but also sympathetic nerve fibers (SNF). Circadian variation and changes in autonomic nervous system activity are involved in angina attacks in patients with vasospastic angina.[14,15] Indeed, surgical sympathectomy has been reported to be effective for the treatment of refractory angina.[16] However, the procedure is invasive in nature and, thus, cannot be performed repeatedly. Currently, catheter-based renal denervation (RDN) has been developed to reduce sympathetic nerve activity,[17,18] which significantly reduced blood pressure (BP) in patients with resistant hypertension.[19–21] Furthermore, RDN is reported to have cardioprotective effects on cardiac myocytes to attenuate cell death and protect against ischemic injury in an animal model.[22] It is, thus, conceivable that RDN could be a therapeutic option for impaired coronary vasomotion after DES implantation through inhibition of the adventitial SNF.

In the present study, we, thus, examined (1) whether DES-induced coronary hyperconstricting responses are associated with enhanced coronary adventitial SNF formation, and if so, (2) whether RDN affects sympathetic autonomic nervous system through the kidney–brain–heart axis, and (3) whether RDN suppresses coronary hyperconstricting responses after DES implantation in pigs in vivo.

Materials and Methods

We conducted 2 experimental protocols. In protocol 1 (Figure 1A), we examined whether DES-induced coronary hyperconstricting responses are associated with enhanced coronary adventitial SNF formation. In protocol 2 (Figure 1B), we examined whether RDN affects sympathetic autonomic nervous system and whether RDN suppresses coronary hyperconstricting responses after DES implantation in pigs in vivo. Detailed Methods are available in the online-only Data Supplement.

Results

Protocol 1: DES Enhances Coronary Adventitial SNF

In protocol 1 (Figure 1A), at 1 month after stent implantation, no significant in-stent restenosis was noted at the stent

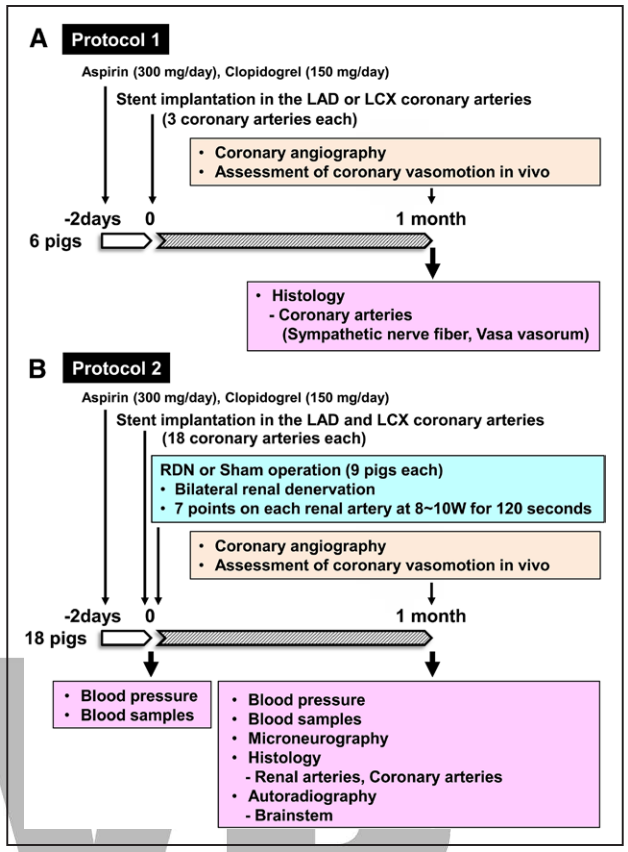

Figure 1. A, Protocol 1: an everolimus-eluting stent (EES) was randomly implanted into the left anterior descending coronary artery (LAD) or the left circumflex coronary artery (LCX) in 6 pigs. At 1 mo after stent implantation, all animals underwent follow-up coronary angiography followed by histological analysis. **B**, Protocol 2: EES were implanted into both the LAD and the LCX in 18 pigs. Subsequently, pigs were randomly assigned to either bilateral renal denervation (RDN) or sham group and underwent each procedure (N=9 each). At 1 mo after the procedure, all animals underwent microneurography and follow-up coronary angiography, followed by histological analysis. Blood pressure and blood analysis were performed before the stent implantation and at 1 mo during follow-up angiography.

implantation sites (Figure 2A). In protocol 1, coronary vasoconstricting responses and histomorphometrical values at the proximal and distal edges in a pig were treated as individual factors (Figure I in the online-only Data Supplement). Coronary vasoconstricting responses to intracoronary serotonin were enhanced at the DES edges compared with the control sites (Figure 2B), and all of them were abolished by pretreatment with hydroxyfasudil (Figure 2C). Quantitative coronary angiography analysis showed that serotonin-induced coronary vasoconstriction was significantly enhanced at the DES edges compared with the control sites (control, 12.8±4.6%; DES, 47.2±3.6%; $P<0.01$; Figure 2D). Masson trichrome staining showed that the coronary adventitial nerve fibers were noted more prominent at the DES edges, as compared with the control sites (Figure 2E and 2J). Indeed, tyrosine hydroxylase (TH) staining showed that the number of TH-positive SNF in the adventitia was significantly increased at the DES edges compared with the control sites ($P<0.01$; Figure 2F, 2K, and 2O). Similarly, the number of vWF-positive

Downloaded from http://atvb.ahajournals.org/ by guest on August 20, 2017

ATVB Arteriosclerosis, Thrombosis, and Vascular Biology FIRST PROOF ONLY

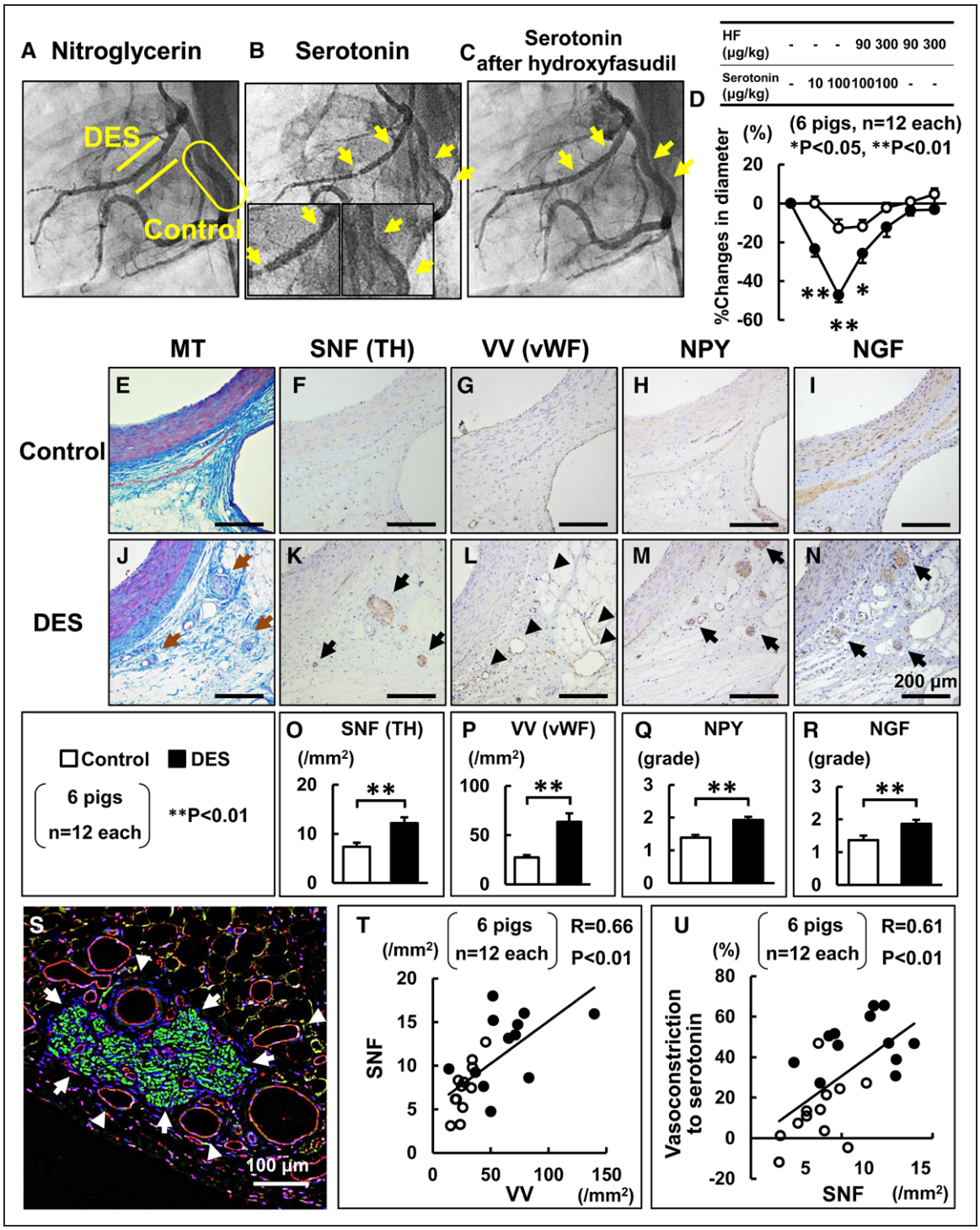

Figure 2. Representative left coronary angiograms after nitroglycerin (10 μg/kg, IC; **A**), serotonin (100 μg/kg, IC) alone (**B**), and serotonin after pretreatment with hydroxyfasudil (HF; 300 μg/kg, IC; **C**) at 1 mo after drug-eluting stent (DES) implantation. Results are presented from a quantitative coronary angiography on coronary vasoconstricting responses to serotonin (10 and 100 μg/kg, IC) before and after HF (90 and 300 μg/kg, IC; **D**). Representative pictures at the stent edges of Masson trichrome (MT) staining (**E** and **J**), immunostainings for sympathetic nerve fiber (SNF; tyrosine hydroxylase [TH]-positive; **F** and **K**), and vasa vasorum (VV; von Willebrand factor [vWF]-positive) stainings (**G** and **L**), neuropeptide Y (NPY; **H** and **M**), and nerve growth factor (NGF) stainings (**I** and **N**). Quantitative/semiquantitative analysis of SNF and VV densities (**O** and **P**) and NPY and NGF expression (**Q** and **R**). Representative pictures at the stent edges of immunofluorescence stainings for SNF (green) and VV (red; **S**). Scale bars represent 200 (**E** through **N**) and 100 μm (**S**). Correlations between the SNF and VV densities (**T**) and between the SNF density and the extent of serotonin (100 μg/kg, IC)-induced coronary vasoconstricting responses at the stent edges (**U**). Yellow bars indicate DES implantation site; yellow ellipse, the control site; brown arrows, nerve fibers; black arrows, SNF; and black arrowheads, VV, respectively. White and black represent the control and the DES groups, respectively. The number of pigs was 6 and the number of coronary artery sites examined was 12 each (both control and DES). Results are expressed as mean±SEM. *P<0.05, **P<0.01 control vs DES.

Downloaded from http://atvb.ahajournals.org/ by guest on August 20, 2017

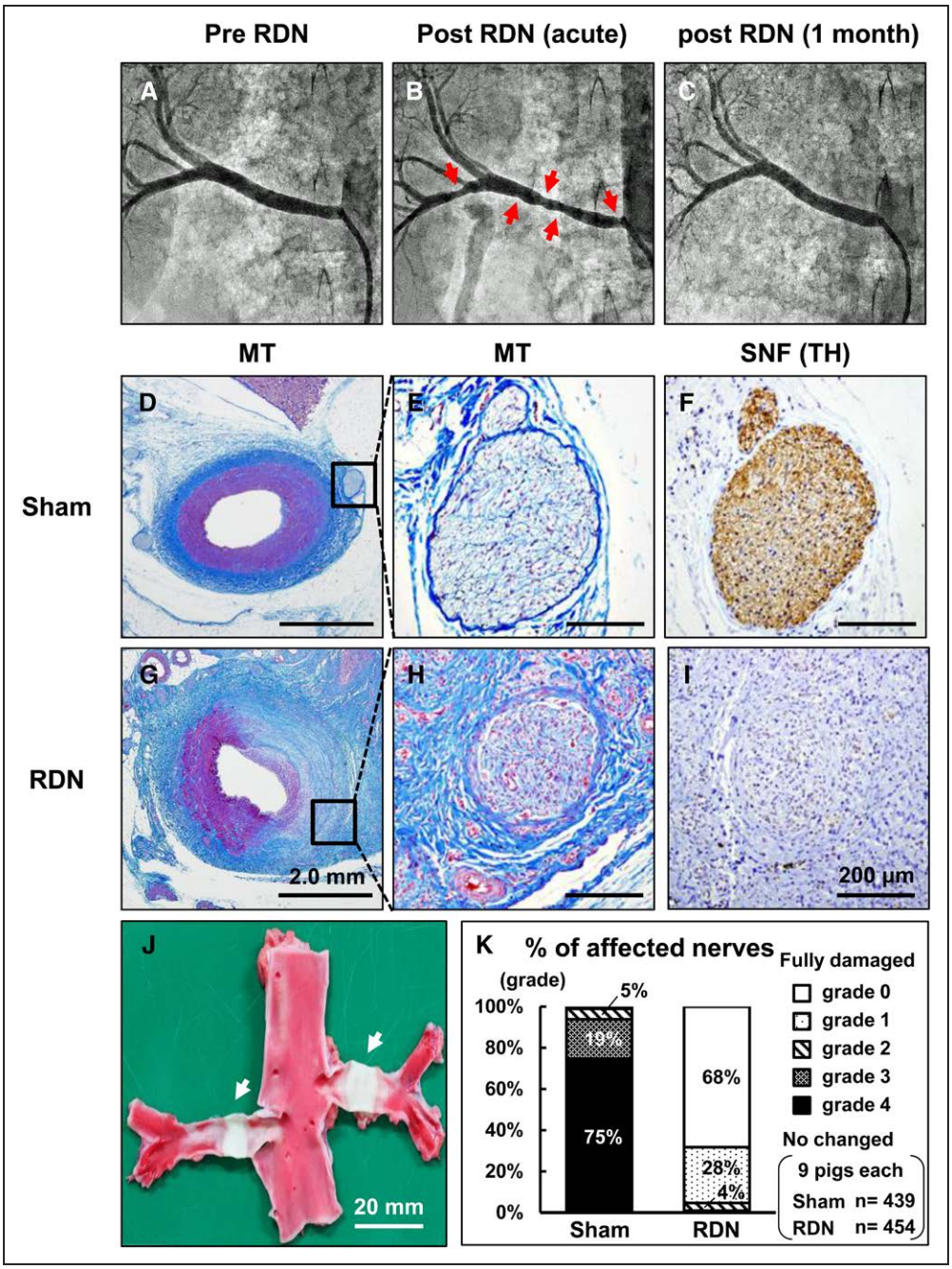

Figure 3. Representative left renal angiograms before renal denervation (RDN; **A**) and immediately after (**B**) and at 1 mo after RDN (**C**). Representative pictures at the renal artery for Masson trichrome (MT) stainings (**D**, **E**, **G**, and **H**), immunostainings for sympathetic nerve fiber (SNF; tyrosine hydroxylase [TH]-positive) stainings (**F** and **I**) at 1 mo after the RDN or sham procedure. Representative picture at the renal artery for 1,3,5-triphenyl tetrazolium chloride staining at 2 h after the RDN procedure (**J**). Percentages of nerve fibers that appeared fully damaged (grade 0), highly damaged (grade 1), mildly damaged (grade 2), almost no changed (grade 3), or no changed (grade 4) assessed by TH staining (**K**). Scale bars represent 2.0 mm (**D** and **G**), 200 μm (**E**, **F**, **H**, and **I**), and 20 mm (**J**). Red arrows indicate notches, and white arrows indicate denervation sites. The number of pigs was 9 each and n represents that of renal nerves examined (both sham and RDN).

microvessels in the adventitia was significantly increased at the DES edges compared with the control sites ($P<0.01$; Figure 2G, 2L, and 2P). Immunoreactivities of both neuropeptide Y (NPY) and nerve growth factor (NGF) predominantly expressed in the adventitial SNF were enhanced at the DES edges compared with the control sites (Figure 2H, 2I, 2M, and 2N). Furthermore, semiquantitative analysis for the extents of NPY and NGF expression in the adventitial SNF showed that both expressions were significantly increased at the DES edges compared with the control sites (all $P<0.01$; Figure 2Q and 2R). Of note, immunofluorescence staining showed that coronary adventitial SNF and VV were closely observed as if they form like a network, and there was a significant positive correlation between the adventitial SNF and VV densities at the stent edges with vasoconstriction sites ($P<0.01$; Figure 2S and 2T). Moreover, there was a significant positive correlation

Downloaded from http://atvb.ahajournals.org/ by guest on August 20, 2017

between the adventitial SNF density at the vasoconstriction sites and the extent of serotonin-induced coronary vasoconstricting responses ($P<0.01$; Figure 2U).

Protocol 2: RDN Inhibits DES-Induced Coronary Hyperconstricting Responses and Enhanced Coronary Adventitial SNF

RDN Procedure

In the RDN procedure, the power output was maintained at 9–10 W during the procedure (Figure IIA in the online-only Data Supplement). The impedance significantly decreased after RDN compared with that before the procedure (pre, 162±1Ω; post, 152±1Ω; n=126; $P<0.01$; Figure IIB in the online-only Data Supplement). The localized temperature was maintained under 50°C without overheating (Figure IIC in the online-only Data Supplement). Immediately after the RDN procedure, renal artery angiography showed no evidence of renal artery thrombus, dissection, or perforation (Figure 3A and 3B). The mean number of notch, which indicated a biological effect of energy delivery on the artery defined as a visible depression in vessel wall at the site of ablation on fluoroscopic image,[23] was 4.5±1.5 per renal artery in the RDN group (n=18). At 1 month after the procedure, there was no evidence of renal artery stenosis, thrombus, dissection, or perforation (Figure 3C).

Histomorphometry of the Renal Artery

At 1 month after the RDN procedure, the renal arteries showed medial fibrosis, suggesting appropriate healing. There was no medial thinning, aneurysm, rupture, or thrombus formation (Figure 3D and 3G). As previously reported,[18] the perivascular nerves showed degenerative change in the RDN

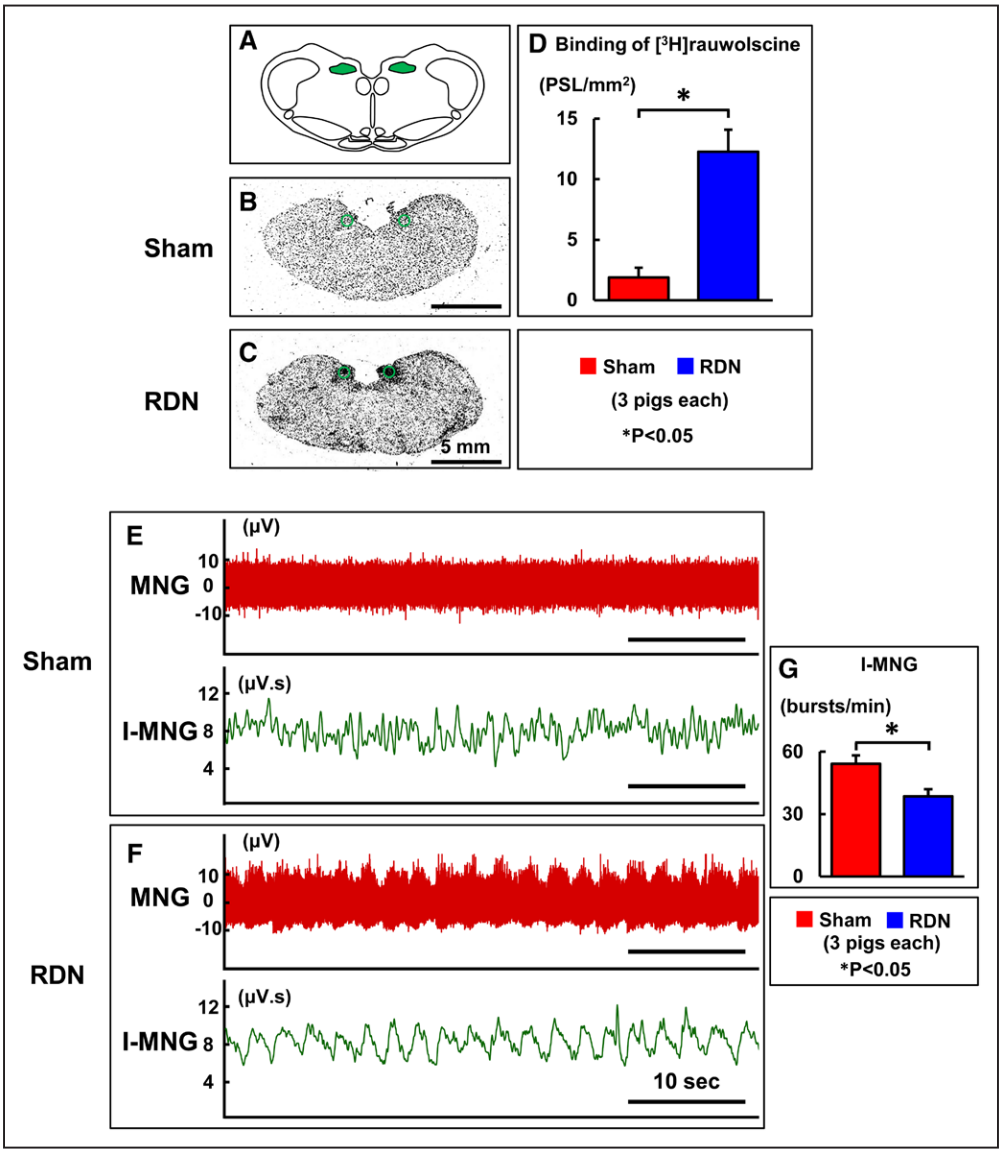

Figure 4. Location of the nucleus tractus solitarius (NTS) regions in the medulla oblongata (**A**). Representative pictures of autoradiogram with [^{3}H]rauwolscine—a specific radioligand for α_2-adrenoceptor binding sites (**B** and **C**). Results are presented from the photostimulated luminescence divided by the regions of interest (ROI) area (**D**). Representative pictures of filtered microneurogram (MNG) and its integrated MNG (I-MNG; **E** and **F**). Green areas indicate NTS regions, and green circles indicate ROI, respectively. Results are presented from I-MNG (**G**). The number of pigs was 3 each (both sham and renal denervation [RDN]). Results are expressed as mean±SEM. *$P<0.05$ sham vs RDN.

Downloaded from http://atvb.ahajournals.org/ by guest on August 20, 2017

group (Figure 3E and 3H). TH staining—a marker of sympathetic nerve viability—showed that >90% renal nerves were damaged in the RDN group (grades 3 and 4; 94%), whereas almost all renal nerves were intact in the sham group (grade 0–2; 99%; Figure 3F, 3I, and 3K). 1,3,5-triphenyl tetrazolium chloride staining at 2 hours after the procedure clearly showed that RDN caused severe damage on the endothelium of bilateral renal arteries (Figure 3J).

In Vitro Autoradiography of the Brain Stem

We performed in vitro autoradiography to evaluate the effect of RDN on [^{3}H]rauwolscine binding to α_2-adrenergic–binding sites in the nucleus tractus solitarius (NTS) regions (Figure 4A through 4C). Because there was no laterality in the NTS regions between the sham and RDN groups (data not shown), the bindings of [^{3}H]rauwolscine were calculated by averaging the bilateral photostimulated luminescence. The extent of the binding of [^{3}H]rauwolscine was significantly higher in the RDN group compared with the sham group (sham, 1.9±1.0 photostimulated luminescence/mm^2; RDN, 12.3±2.7 photostimulated luminescence/mm^2; P<0.05; Figure 4D).

Effects of RDN on Muscle Sympathetic Nerve Activity

At 1 month after RDN or sham procedure, filtered microneurogram and its integrated microneurogram (an established and reliable parameter reflecting sympathetic nerve activity) were recorded (Figure 4E through 4G).[24,25] Integrated microneurogram showed that muscle sympathetic nerve activity was significantly attenuated in the RDN group compared with the sham group (sham, 54±4 bursts/min; RDN, 39±3 bursts/min; P<0.05).

Effects of RDN on Arterial BP and Heart Rate

At baseline, systolic (SBP), diastolic, and mean BP and HR were all comparable between the sham and the RDN groups (Table 1). SBP increased from baseline to 1 month after the procedure in the sham group (before the procedure, 95±4 mm Hg; 1 month after the procedure, 115±5 mm Hg; change over time, 19±4 mm Hg P<0.01 [by using pared, 2-sided Student t test]). In contrast, in the RDN group, there were no significant changes (before the procedure, 97±4 mm Hg; 1 month after the procedure, 102±3 mm Hg; change over time, 5±6 mm Hg; P=0.43). In contrast, although diastolic and mean BP also increased in both groups, there were no significant differences in the extents of BP increase between the 2 groups.

Effects of RDN on Blood Analysis

At baseline, serum levels of electrolytes, renal function, and renin–angiotensin–aldosterone system were all comparable between the sham and the RDN groups (Table 2). Serum levels of potassium, chloride, creatinine, and aldosterone remained unchanged from baseline to 1 month after the procedure between the 2 groups. However, the extent of the increase in plasma renin activity was significantly lower in the RDN group compared with the sham group (P<0.05). In addition, the extent of increase in sodium and urea nitrogen were also significantly lower in the RDN group compared with the sham group (all P<0.05).

Stent Implantation

There were no significant differences in the procedural parameters for stent implantation between the sham and the RDN groups, including target vessel diameter, stent diameter, or overstretch ratio (Table 3).

Table 1. Arterial Blood Pressure and Heart Rate Before and 1 mo After Sham or RDN Procedure

	Sham (N=9)	RDN (N=9)	*P* Value
Before			
SBP, mm Hg	95±4	97±4	0.73
Diastolic BP, mm Hg	55±4	54±3	0.81
Mean BP, mm Hg	75±5	72±4	0.58
Heart rate, bpm	103±6	97±4	0.39
1 mo after			
SBP, mm Hg	115±5	102±3	<0.05
Diastolic BP, mm Hg	63±4	58±3	0.30
Mean BP, mm Hg	84±4	76±3	0.17
Heart rate, bpm	103±5	97±4	0.28
Change over time			
ΔSBP, mm Hg	19±4	5±6	<0.05
ΔDiastolic BP, mm Hg	8±4	4±4	0.49
ΔMean BP, mm Hg	9±4	5±5	0.52
ΔHeart rate, bpm	1±4	1±4	0.95

The number N represents that of pigs. Results are expressed as mean±SEM. Δ indicates the difference between before and 1 mo after the procedure. BP indicates blood pressure; RDN, renal denervation; and SBP, systolic blood pressure.

Effects of RDN on Coronary Vasomotion After Stent Implantation

At 1 month after stent implantation, no in-stent restenosis was noted (Figure 5A and 5D). Notably, coronary vasoconstricting responses to intracoronary serotonin were attenuated at the proximal and distal stent edges in the RDN group compared with the sham group (Figure 5B and 5E), all of which were abolished by pretreatment with hydroxyfasudil (Figure 5C and 5F). Quantitative coronary angiography analysis demonstrated that serotonin-induced coronary vasoconstriction was significantly attenuated in the RDN group compared with the sham group (sham, 30.2±3.5%; RDN, 14.4±3.3%; P<0.01; Figure 5G). In contrast, endothelium-dependent and independent coronary vasodilating responses to nitroglycerin and bradykinin were all comparable between the 2 groups, regardless of the presence or absence of N^G-monomethyl-L-arginine (Table 4).

Histomorphometry of the Stent Edges

Histomorphometric parameters at the stent edges were all comparable between the sham and the RDN groups (Table 5).

Effects of RDN on Coronary Adventitial SNF and VV Formation at the Stent Edges

At the stent edges, Masson trichrome stainings showed that the number of nerve fibers in the coronary adventitia was smaller in the RDN group, as compared with the sham group (Figure 6A and 6F). Indeed, TH staining showed that the number of TH-positive SNF in the adventitia was significantly reduced in the RDN group, as compared with the sham group

Downloaded from http://atvb.ahajournals.org/ by guest on August 20, 2017

ATVB Arteriosclerosis, Thrombosis, and Vascular Biology FIRST PROOF ONLY

Table 2. Blood Parameters Before and 1 mo After the Sham or RDN Procedure

	Sham (N=6)		RDN (N=6)	
	Before	1 mo	Before	1 mo
Na, mEq/L	141±1	147±2	147±3	144±2
K, mEq/L	4.2±0.1	4.4±0.1	4.3±0.1	4.6±1.1
Cl, mEq/L	103±1	106±1	106±2	105±1
BUN, mg/dL	11.1±1.1	17.7±1.8	13.6±1.3	16.3±0.6
Scr, mg/dL	0.9±0.0	1.1±0.1	0.9±0.1	1.1±0.1
PRA, ng·dL·h	1.3±0.4	1.8±0.6	1.2±0.5	0.7±0.1
ALD, ng/dL	2.6±0.4	2.8±0.6	2.8±0.7	2.7±0.7
		Sham (N=6)	RDN (N=6)	*P* Value
ΔNa, mEq/L		5.1±2.4	−2.6±2.0	<0.05
ΔK, mEq/L		0.2±0.2	0.3±0.1	0.53
ΔCl, mEq/L		3.4±1.4	−1.1±1.8	0.07
ΔBUN, mg/dL		6.6±1.0	2.6±1.0	<0.05
ΔScr, mg/dL		0.2±0.1	0.2±0.0	0.33
ΔPRA, ng·dL·h		0.6±0.3	−0.5±0.4	<0.05
ΔALD, ng/dL		0.2±0.3	−0.2±0.3	0.50

The number N represents that of pigs. Results are expressed as mean±SEM. Δ indicates the difference between before and 1 mo after the procedure. ALD indicates plasma levels of aldosterone; BUN, blood urea nitrogen; Cl, plasma chloride level; K, potassium; Na, sodium; PRA, plasma renin activity; RDN, renal denervation; and Scr, serum creatinine.

(*P*<0.01; Figure 6B, 6G, and 6K). Similarly, the number of vWF-positive VV in the adventitia was significantly reduced in the RDN group compared with the sham group (*P*<0.01; Figure 6C, 6H, and 6L). Furthermore, semiquantitative analysis for the extents of NPY and NGF expression in the adventitial SNF showed that both expressions were significantly decreased in the RDN group compared with the sham group (all *P*<0.01; Figure 6D, 6E, 6I, 6J, 6M, and 6N). Importantly, there was a significant positive correlation between the adventitial SNF and VV densities at the stent edge vasoconstriction sites (*P*<0.01; Figure 6O).

Table 3. Procedural Parameters

	Sham	RDN	*P* Value
Target vessel (LAD/LCX)	9/9	9/9	…
Target vessel diameter, mm	2.5±0.1	2.6±0.2	0.57
Stent diameter, mm	2.8±0.1	2.8±0.1	0.75
Stent length, mm	16.0±0.0	16.0±0.0	…
Overstretch ratio	1.1±0.0	1.1±0.0	0.32
Distal overstretch ratio	1.1±0.0	1.1±0.0	0.43
Maximum inflation pressure, atm	17.1±1.0	18.0±0.6	0.59

Results are expressed as mean±SEM. Stent diameter was calculated by averaging the diameters at the proximal edge, mid portion, and distal edge of the stented coronary artery. Overstretch ratio was calculated as the stent diameter divided by target vessel diameter. Distal overstretch ratio was calculated as the distal stent diameter divided by distal reference vessel diameter. LAD indicates left anterior descending coronary artery; LCX, left circumflex coronary arteries; and RDN, renal denervation.

Effects of RDN on Adventitial Inflammatory Changes at the Stent Edges

At the stent edge portions, infiltration of inflammatory cells in the adventitia was less in the RDN group compared with the sham group (Figure IIIA and IIIE in the online-only Data Supplement). Indeed, the number of CD68-positive macrophages (Figure IIIB, IIIF, and IIII in the online-only Data Supplement) and interleukin-1β–positive cells (Figure IIIC, IIIG, and IIIJ in the online-only Data Supplement) were significantly decreased at the edges in the RDN group compared with the sham group (*P*<0.05 for macrophages and *P*<0.01 for interleukin-1β–positive cells). Toluidine blue-positive mast cells were also less noted at the edges in the RDN group compared with the sham group (*P*<0.01; Figure IIID, IIIH, and IIIK in the online-only Data Supplement).

Effects of RDN on Rho-Kinase Activity at the Stent Edges

Immunoreactivities for Rho-associated coiled coil containing protein kinase 1/2 and phosphorylated myosin phosphatase target subunit-1 (a marker of Rho-kinase activity)[26] were predominantly noted in the medial vascular smooth muscle cells. In the semiquantitative analysis, the extent of Rho-associated coiled coil containing protein kinase 1/2 expressions and Rho-kinase activation (phosphorylated myosin phosphatase target subunit-1) at the stent edges were significantly lower in the RDN group compared with the sham group (all *P*<0.05; Figure IIIM through IIIO, IIIQ through IIIS, and IIIT through IIIV in the online-only Data Supplement).

Discussion

The major findings of the present study were that (1) enhanced SNF and VV formation were noted at the edges of DES implantation sites with enhanced coronary vasoconstricting responses, (2) NTS regions in the central nervous system were influenced by the RDN procedure with resultant decrease in BP and reduced activity of plasma renin and muscle sympathetic nerves, (3) RDN attenuated coronary vasomotion abnormalities after DES implantation in pigs in vivo, (4) RDN also attenuated SNF, VV, and inflammation in the coronary adventitia and Rho-kinase activation after DES implantation, and (5) there were significant correlations between morphological changes (eg, SNF, VV, and inflammatory cell infiltration) and functional changes of the coronary artery (eg, hyperconstricting responses).

Coronary Adventitial SNF and DES-Induced Coronary Hyperconstricting Responses

The present study demonstrates for the first time in pigs that coronary adventitial SNF were enhanced associated with VV growth at the stent implantation sites. Of note, immunofluorescence staining revealed that coronary adventitial SNF and VV are closely present like a tangle. In addition, enhanced coronary adventitial SNF formation was positively correlated with the extent of serotonin-induced coronary vasoconstriction, suggesting that sympathetic hyperactivity is involved in the pathogenesis of

Downloaded from http://atvb.ahajournals.org/ by guest on August 20, 2017

ATVB Arteriosclerosis, Thrombosis, and Vascular Biology FIRST PROOF ONLY

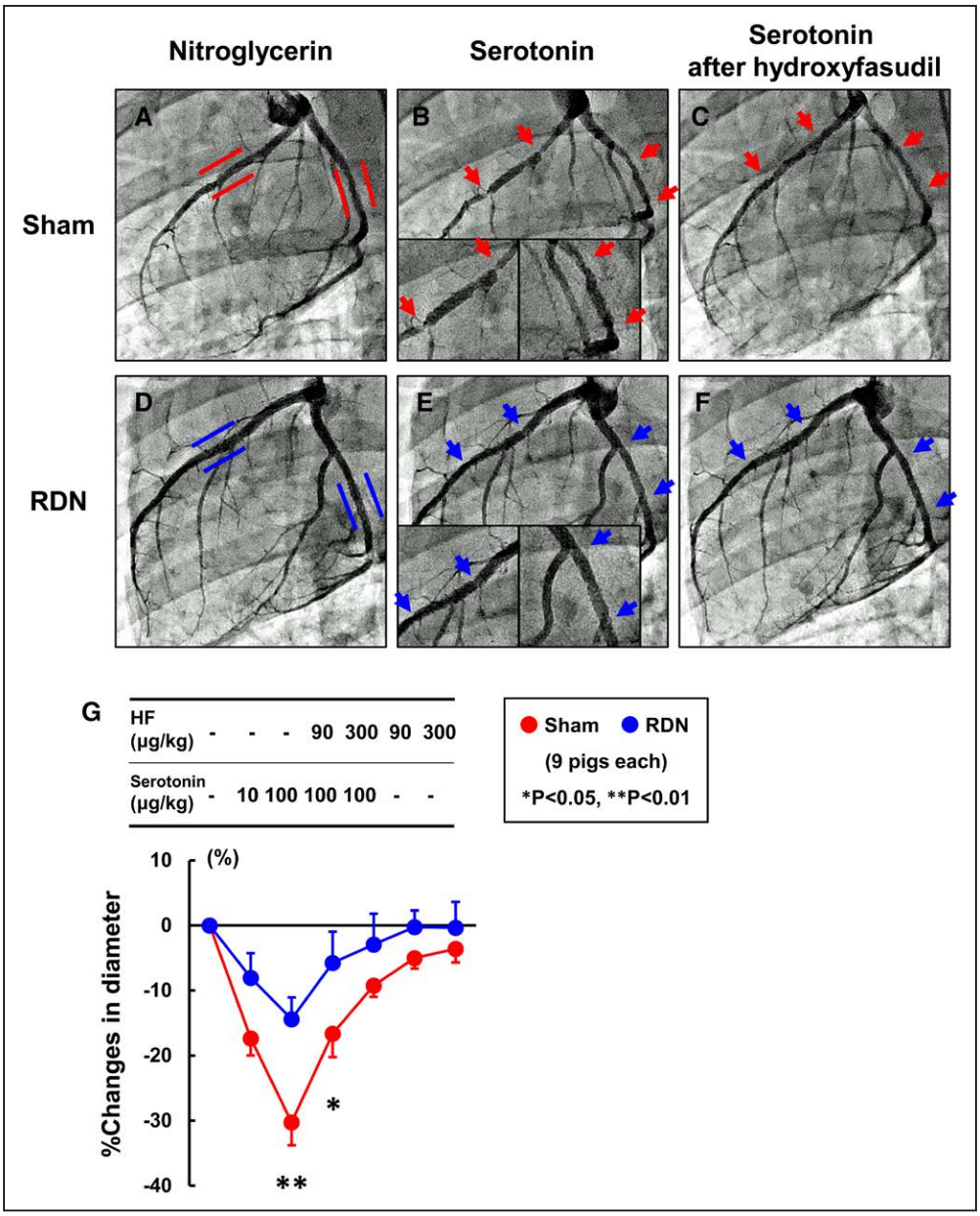

Figure 5. Representative left coronary angiograms after nitroglycerin (10 μg/kg, IC; **A** and **D**), serotonin (100 μg/kg, IC) alone (**B** and **E**), and serotonin after pretreatment with hydroxyfasudil (HF; 300 μg/kg, IC; **C** and **F**) 1 mo after stent implantation. Results are presented from a quantitative coronary angiography on coronary vasoconstricting responses to serotonin (10 and 100 μg/kg, IC) before and after HF (90 and 300 μg/kg, IC; **G**). The number of pigs was 9 each (both sham and renal denervation [RDN]). Results are expressed as mean±SEM. **P*<0.05, ***P*<0.01 sham vs RDN.

coronary hyperconstricting responses after DES implantation. Furthermore, we showed that the expressions of the neuromodulators, NPY (an angiogenic factor), and NGF (a neurogenic factor) in the coronary adventitial SNFs were enhanced at the DES edges, suggesting possible interactions between VV and SNF. Indeed, recent studies suggest that peripheral nervous system directly influences blood vessel pattern resulting in nerve–artery alignment.[27,28] Thus, it is possible that augmented SNF is involved in the VV formation with resultant coronary hyperconstricting responses at the DES-implanted site. These results suggest that modulation of autonomic nerve activity with catheter-based RDN has potential therapeutic effects to improve coronary vasomotion abnormalities through inhibition of VV formation and inflammatory cell recruitment.

Inhibitory Effects of RDN on Sympathetic Nervous System

We first validated the damage by RDN in bilateral renal arteries. Renal artery angiography showed several notches immediately after RDN, which indicated a biological effect of energy delivery on the artery.[23] Sub analysis of the simplicity HTN-3 trial demonstrated that patients with resistant hypertension who received >14 ablation attempts had significantly greater reduction in home and office SBP, whereas those who received <9 ablation attempts did not have reduction in BP.[29] In line with

Downloaded from http://atvb.ahajournals.org/ by guest on August 20, 2017

Table 4. Coronary Vasodilating Responses

	Sham (N=9)	RDN (N=9)	*P* Value
Nitroglycerin, %	5.3±1.5	3.8±2.4	0.60
Bradykinin, %	7.4±3.0	7.2±1.9	0.96
Bradykinin after L-NMMA, %	4.2±1.7	5.5±2.1	0.63

The number N represents that of pigs. Results are expressed as mean±SEM. Coronary vasodilating responses were evaluated by quantitative coronary angiography in response to nitroglycerin (10 μg/kg, IC) and bradykinin (0.1 μg/kg, IC) before and after L-NMMA (1 mg/kg, IC) at 1 mo. Percentage changes in diameter are expressed as changes in diameter from the baseline level (contrast medium only). The mean value of vasodilating responses at the proximal and the distal stent edges are presented. L-NMMA indicates N^G-monomethyl-L-arginine; and RDN, renal denervation.

this finding, we performed frequent ablation attempts (14× per pig) with monitoring power output, localized impedance, and localized temperature. We confirmed successful reduction in localized impedance after RDN without overheating and no late stenosis at the ablation sites. Furthermore, we histologically confirmed that RDN caused marked damages of SNF surrounding the renal arteries.

We then examined the effects of RDN on brain function by using in vitro autoradiography. In the present study, we were able to demonstrate for the first time the brain images showing functional alterations in response to the RDN procedure. Strikingly, the [^{3}H]rauwolscine binding to α_2-adrenergic receptor in the NTS regions was significantly upregulated in the RDN group. NTS is the area of the brain stem that plays a key role in the regulation and integration of autonomic nerves activities.[30] It is known that renal afferent input interacts with cardiovascular afferent input at neurons in the NTS.[31] The NTS also receives baroreceptor afferents and a dense noradrenergic input.[32] Notably, hypertensive animals show downregulation of the [^{3}H]rauwolscine binding to α_2-adrenergic receptor in the NTS regions.[30] In contrast, stimulation of α_2 receptor within the NTS promotes a strong hypotensive response.[33,34] Thus, RDN may cause (1) upregulation of α_2 receptor in NTS, (2) downregulation of sympathetic nerve activity, and subsequently (3) suppression of DES-induced coronary hyperconstricting responses and attenuation of SNF in coronary adventitia. However, detailed mechanisms remain to be elucidated in future studies.

We also examined the effects of RDN on systemic autonomic nerve activity. RDN significantly decreased levels of plasma renin activity indicate possible suppression of the renin–angiotensin–aldosterone system by RDN. Furthermore, a reduction in muscle sympathetic nerve activity after RDN procedure, as assessed in the femoral nerve using microneurography, highlighted the possibility that inhibition of afferent bilateral renal nerve activity could contribute to a decrease in central sympathetic drive through the NTS pathway.

Table 5. Histomorphometry at the Stent Edges

	Sham (N=9)	RDN (N=9)	*P* Value
Lumen diameter, mm	1.4±0.1	1.4±0.1	0.47
Intimal+medial thickness, mm	0.2±0.0	0.2±0.0	0.47
Intimal+medial area, mm^2	0.9±0.1	1.0±0.1	0.49
Adventitial area, mm^2	1.1±0.1	1.2±0.1	0.35

The number N represents that of pigs. Results are expressed as mean±SEM. The adventitial area was calculated by the following formula: area outside the EEL within a distance of the thickness of neointima plus media–EEL area. EEL indicates external elastic lamina; and RDN, renal denervation.

Effects of RDN on BP and HR

In porcine models with hypertension, inhibitory effect of RDN on SBP was noted.[35,36] In the present study with normotensive pigs, RDN also significantly decreased SBP compared with the sham group at 1 month after the procedure, although the extent of SBP changes during 1 month remained unchanged in the RDN group compared with the sham group. In humans, procedural performance, such as the frequency of ablation, might influence the degree of SBP reduction after RDN.[29]

In the present study, RDN did not significantly affect HR. In patients with resistant hypertension who underwent >14 ablations, RDN caused significant reduction in HR (−4.5 bpm) at 6 months after the procedure.[29] However, it has been reported that RDN did not significantly affect HR in porcine models.[35,36] Thus, the mechanisms and discrepancy of the effects of RDN on BP and HR between pigs and humans remain to be examined in future studies.

Effects of RDN on Coronary Adventitia and Vasomotion

It is important to demonstrate the key roles of the adventitia for the assessment of the effect of RDN on coronary vasomotion abnormalities. Signals originating from the adventitia play essential roles in the regulation of physiology and vascular disease, such as coronary artery spasm.[10] The adventitia harbors a variety of components that potently modulate vascular tone, including inflammatory cells, VV, and importantly SNF.[37] Coronary spasm can be induced by stimuli, such as cold pressor test, that increases sympathetic outflow.[38] Circadian variation of autonomic nervous system activity in angina attacks in patients with vasospastic angina also suggests an involvement of the coronary adventitial SNF.[15] Thus, the present findings suggest that SNF in the adventitia is a potential therapeutic target for coronary vasomotion abnormalities.

VV could be a conduit of inflammatory cells to the adventitia.[37] We also have recently demonstrated that enhanced VV formation in the coronary adventitia is associated with DES-induced coronary hyperconstricting responses in pigs in vivo[12] and coronary spasm in humans.[13] In the present study, it is considered that RDN reduced SNF and VV formation after DES implantation, which could inhibit the recruitment of inflammatory cells and advanced inflammation. The adventitia is also in contact with and is completely surrounded by the media that is predominantly composed of vascular smooth muscle cells that regulate vasomotor function. Indeed, we demonstrated that Rho-kinase activation of vascular smooth muscle cells in response to the adventitial inflammation plays important roles in the pathogenesis of coronary spasm in animals.[11] These findings provide an important insight into the adventitia as a potential therapeutic target for coronary vasomotion abnormalities.

Downloaded from http://atvb.ahajournals.org/ by guest on August 20, 2017

ATVB Arteriosclerosis, Thrombosis, and Vascular Biology FIRST PROOF ONLY

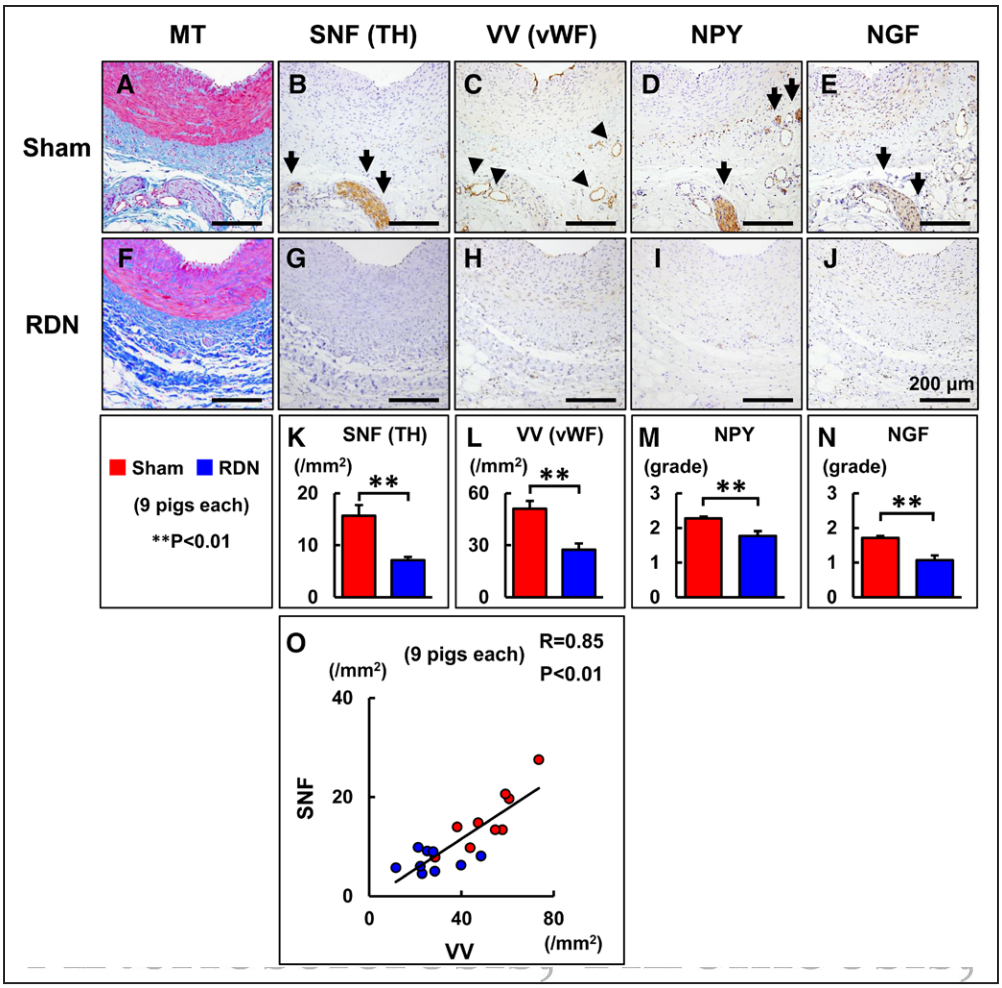

Figure 6. Representative pictures at the stent edges for Masson trichrome (MT; **A** and **F**), immunostainings for sympathetic nerve fiber (SNF; tyrosine hydroxylase [TH]-positive; **B** and **G**), vasa vasorum (VV; von Willebrand factor [vWF]-positive; **C** and **H**), neuropeptide Y (NPY; **D** and **I**), and nerve growth factor (NGF) stainings (**E** and **J**). Scale bars represent 200 μm. Arrows indicate SNF, and arrow heads indicate VV, respectively. Quantitative/semiquantitative analysis of SNF and VV densities (**K** and **L**) and NPY and NGF expression (**M** and **N**). Correlations between the SNF and VV densities at the stent edges (**O**). The number of pigs was 9 each (both sham and RDN) Results are expressed as mean±SEM. ***P*<0.01 sham vs RDN.

Arteriosclerosis, Thrombosis, and Vascular Biology
FIRST PROOF ONLY

However, from a clinical point of view, it is difficult to deliver pharmacological agents or genes into the coronary adventitia in humans. Based on the present findings, it is conceivable that RDN could be used as a treatment option to modify the adventitial SNF associated with adjacent VV and inflammatory cells and resultant consequences of the disorder.

Translational Perspective

Surgical sympathectomy has been reported to be effective for the treatment of refractory angina,[16] although the procedure is invasive in nature and, thus, cannot be performed repeatedly. Currently, intractable vasospastic angina and unremitting angina even after successful percutaneous coronary intervention are also emerging therapeutic targets.[4–6] In the present study, we were able to demonstrate that RDN ameliorates coronary hyperconstricting responses after DES implantation in pigs in vivo through the possible kidney–brain–heart axis (Graphic Abstract). Thus, RDN could be used as a treatment option to modify the adventitial SNF associated with adjacent VV and inflammatory cells and resultant vasospastic disorder.

Study Limitations

Several limitations should be mentioned for the present study. First, time course and interactions between SNF and VV formation after DES implantation and RDN procedure remain to be elucidated. Recent studies suggest that some neurotrophic factors, including NPY and NGF, have angiogenic effects and stimulate regeneration and maturation of perivascular nerves.[27,39] Second, in the present study, we only examined the effects of RDN procedure in a prevention protocol. Thus, it remains to be examined whether RDN, as a secondary prevention, improves established coronary vasomotion abnormalities after DES implantation. Third, we used serotonin to examine coronary vasoconstricting responses, as previously described.[9,12,26] Although acetylcholine is most frequently used to provoke coronary artery spasm in the clinical setting, serotonin may better mimic spontaneous coronary spasm in humans than acetylcholine.[40] Fourth, we used normal pig with neither impaired endothelial function nor abundant atherosclerotic burden. Thus, caution should be paid when applying the present results to humans.

Downloaded from http://atvb.ahajournals.org/ by guest on August 20, 2017

Conclusions

The present study demonstrates that bilateral RDN ameliorates coronary hyperconstricting responses after DES implantation in pigs in vivo through suppression of the kidney–brain–heart axis, including suppressions of coronary adventitial SNF, VV formation, inflammation, and Rho-kinase activation, suggesting that RDN is a novel therapeutic option for refractory angina.

Acknowledgments

We thank Y. Watanabe and A. Nishihara for their excellent technical assistance and Asahi Kasei Pharma for providing hydroxyfasudil.

Sources of Funding

This work was supported, in part, by the grants-in-aid for the Scientific Research (18890018) and the Global COE Project (F02) and the grants-in-aid (H22-Shinkin-004) from the Japanese Ministry of Education, Culture, Sports, Science, and Technology, Tokyo, Japan, the grant for young investigators of translational research from Tohoku University Hospital, and the grants-in-aid by a Sakakibara Memorial Research Grant from the Japan Research Promotion Society for Cardiovascular Diseases.

Disclosures

None.

References

1. Lüscher TF, Steffel J, Eberli FR, Joner M, Nakazawa G, Tanner FC, Virmani R. Drug-eluting stent and coronary thrombosis: biological mechanisms and clinical implications. *Circulation*. 2007;115:1051–1058. doi: 10.1161/CIRCULATIONAHA.106.675934.
2. Aizawa K, Yasuda S, Takahashi J, Takii T, Kikuchi Y, Tsuburaya R, Ito Y, Ito K, Nakayama M, Takeda M, Shimokawa H. Involvement of rho-kinase activation in the pathogenesis of coronary hyperconstricting responses induced by drug-eluting stents in patients with coronary artery disease. *Circ J*. 2012;76:2552–2560.
3. Togni M, Windecker S, Cocchia R, Wenaweser P, Cook S, Billinger M, Meier B, Hess OM. Sirolimus-eluting stents associated with paradoxic coronary vasoconstriction. *J Am Coll Cardiol*. 2005;46:231–236. doi: 10.1016/j.jacc.2005.01.062.
4. Ong P, Athanasiadis A, Perne A, Mahrholdt H, Schäufele T, Hill S, Sechtem U. Coronary vasomotor abnormalities in patients with stable angina after successful stent implantation but without in-stent restenosis. *Clin Res Cardiol*. 2014;103:11–19. doi: 10.1007/s00392-013-0615-9.
5. Tsuburaya R, Takahashi J, Nakamura A, et al; NOVEL Investigators. Beneficial effects of long-acting nifedipine on coronary vasomotion abnormalities after drug-eluting stent implantation: the NOVEL study. *Eur Heart J*. 2016;37:2713–2721. doi: 10.1093/eurheartj/ehw256.
6. Serruys PW, Chevalier B, Dudek D, et al. A bioresorbable everolimus-eluting scaffold versus a metallic everolimus-eluting stent for ischaemic heart disease caused by de-novo native coronary artery lesions (ABSORB II): an interim 1-year analysis of clinical and procedural secondary outcomes from a randomised controlled trial. *Lancet*. 2015;385:43–54. doi: 10.1016/S0140-6736(14)61455-0.
7. Shimokawa H, Sunamura S, Satoh K. RhoA/Rho-kinase in the cardiovascular system. *Circ Res*. 2016;118:352–366. doi: 10.1161/CIRCRESAHA.115.306532.
8. Kandabashi T, Shimokawa H, Miyata K, Kunihiro I, Kawano Y, Fukata Y, Higo T, Egashira K, Takahashi S, Kaibuchi K, Takeshita A. Inhibition of myosin phosphatase by upregulated rho-kinase plays a key role for coronary artery spasm in a porcine model with interleukin-1beta. *Circulation*. 2000;101:1319–1323.
9. Tsuburaya R, Yasuda S, Shiroto T, Ito Y, Gao JY, Aizawa K, Kikuchi Y, Ito K, Takahashi J, Ishibashi-Ueda H, Shimokawa H. Long-term treatment with nifedipine suppresses coronary hyperconstricting responses and inflammatory changes induced by paclitaxel-eluting stent in pigs in vivo: possible involvement of Rho-kinase pathway. *Eur Heart J*. 2012;33:791–799. doi: 10.1093/eurheartj/ehr145.
10. Shimokawa H. 2014 Williams Harvey lecture: importance of coronary vasomotion abnormalities-from bench to bedside. *Eur Heart J*. 2014;35:3180–3193. doi: 10.1093/eurheartj/ehu427.
11. Shimokawa H, Ito A, Fukumoto Y, Kadokami T, Nakaike R, Sakata M, Takayanagi T, Egashira K, Takeshita A. Chronic treatment with interleukin-1 beta induces coronary intimal lesions and vasospastic responses in pigs in vivo. The role of platelet-derived growth factor. *J Clin Invest*. 1996;97:769–776. doi: 10.1172/JCI118476.
12. Nishimiya K, Matsumoto Y, Shindo T, Hanawa K, Hasebe Y, Tsuburaya R, Shiroto T, Takahashi J, Ito K, Ishibashi-Ueda H, Yasuda S, Shimokawa H. Association of adventitial vasa vasorum and inflammation with coronary hyperconstriction after drug-eluting stent implantation in pigs in vivo. *Circ J*. 2015;79:1787–1798. doi: 10.1253/circj.CJ-15-0149.
13. Nishimiya K, Matsumoto Y, Takahashi J, Uzuka H, Wang H, Tsuburaya R, Hao K, Ohyama K, Odaka Y, Miyata S, Ito K, Shimokawa H. Enhanced adventitial vasa vasorum formation in patients with vasospastic angina: assessment with OFDI. *J Am Coll Cardiol*. 2016;67:598–600. doi: 10.1016/j.jacc.2015.11.031.
14. Lanza GA, Pedrotti P, Pasceri V, Lucente M, Crea F, Maseri A. Autonomic changes associated with spontaneous coronary spasm in patients with variant angina. *J Am Coll Cardiol*. 1996;28:1249–1256. doi: 10.1016/S0735-1097(96)00309-9.
15. Nihei T, Takahashi J, Tsuburaya R, Ito Y, Shiroto T, Hao K, Takagi Y, Matsumoto Y, Nakayama M, Miyata S, Sakata Y, Ito K, Shimokawa H. Circadian variation of Rho-kinase activity in circulating leukocytes of patients with vasospastic angina. *Circ J*. 2014;78:1183–1190.
16. Meller ST, Gebhart GF. A critical review of the afferent pathways and the potential chemical mediators involved in cardiac pain. *Neuroscience*. 1992;48:501–524.
17. Mahfoud F, Lüscher TF, Andersson B, et al. Expert consensus document from the European Society of Cardiology on catheter-based renal denervation. *Eur Heart J*. 2013;34:2147–2157. doi: 10.1093/eurheartj/eht154.
18. Cohen-Mazor M, Mathur P, Stanley JR, Mendelsohn FO, Lee H, Baird R, Zani BG, Markham PM, Rocha-Singh K. Evaluation of renal nerve morphological changes and norepinephrine levels following treatment with novel bipolar radiofrequency delivery systems in a porcine model. *J Hypert*. 2014:32:1678–1691; discussion 1691–1692.
19. Mahfoud F, Bakris G, Bhatt DL, Esler M, Ewen S, Fahy M, Kandzari D, Kario K, Mancia G, Weber M, Böhm M. Reduced blood pressure-lowering effect of catheter-based renal denervation in patients with isolated systolic hypertension: data from SYMPLICITY HTN-3 and the global SYMPLICITY registry. *Eur Heart J*. 2017;38:93–100. doi: 10.1093/eurheartj/ehw325.
20. Böhm M, Mahfoud F, Ukena C, Hoppe UC, Narkiewicz K, Negoita M, Ruilope L, Schlaich MP, Schmieder RE, Whitbourn R, Williams B, Zeymer U, Zirlik A, Mancia G; GSR Investigators. First report of the global SYMPLICITY registry on the effect of renal artery denervation in patients with uncontrolled hypertension. *Hypertension*. 2015;65:766–774. doi: 10.1161/HYPERTENSIONAHA.114.05010.
21. Azizi M, Pereira H, Hamdidouche I, et al; DENERHTN Investigators. Adherence to antihypertensive treatment and the blood pressure-lowering effects of renal denervation in the renal denervation for hypertension (DENERHTN) trial. *Circulation*. 2016;134:847–857. doi: 10.1161/CIRCULATIONAHA.116.022922.
22. Polhemus DJ, Gao J, Scarborough AL, Trivedi R, McDonough KH, Goodchild TT, Smart F, Kapusta DR, Lefer DJ. Radiofrequency renal denervation protects the ischemic heart via inhibition of GRK2 and increased nitric oxide signaling. *Circ Res*. 2016;119:470–480. doi: 10.1161/CIRCRESAHA.115.308278.
23. Bhatt DL, Kandzari DE, O'Neill WW, D'Agostino R, Flack JM, Katzen BT, Leon MB, Liu M, Mauri L, Negoita M, Cohen SA, Oparil S, Rocha-Singh K, Townsend RR, Bakris GL; SYMPLICITY HTN-3 Investigators. A controlled trial of renal denervation for resistant hypertension. *N Engl J Med*. 2014;370:1393–1401. doi: 10.1056/NEJMoa1402670.
24. Nakamura T, Kawahara K, Kusunoki M, Feng Z. Microneurography in anesthetized rats for the measurement of sympathetic nerve activity in the sciatic nerve. *J Neurosci Methods*. 2003;131:35–39.
25. Schlaich MP, Sobotka PA, Krum H, Lambert E, Esler MD. Renal sympathetic-nerve ablation for uncontrolled hypertension. *N Engl J Med*. 2009;361:932–934. doi: 10.1056/NEJMc0904179.
26. Nishimiya K, Matsumoto Y, Uzuka H, Ogata T, Hirano M, Shindo T, Hasebe Y, Tsuburaya R, Shiroto T, Takahashi J, Ito K, Shimokawa H. Beneficial effects of a novel bioabsorbable polymer coating on enhanced coronary vasoconstricting responses after drug-eluting stent implantation in pigs in vivo. *JACC Cardiovasc Interv*. 2016;9:281–291. doi: 10.1016/j.jcin.2015.09.041.

Downloaded from http://atvb.ahajournals.org/ by guest on August 20, 2017

ATVB Arteriosclerosis, Thrombosis, and Vascular Biology FIRST PROOF ONLY

27. Asanome A, Kawabe J, Matsuki M, Kabara M, Hira Y, Bochimoto H, Yamauchi A, Aonuma T, Takehara N, Watanabe T, Hasebe N. Nerve growth factor stimulates regeneration of perivascular nerve, and induces the maturation of microvessels around the injured artery. *Biochem Biophys Res Commun*. 2014;443:150–155. doi: 10.1016/j.bbrc.2013.11.070.
28. Hao L, Zou Z, Tian H, Zhang Y, Song C, Zhou H, Liu L. Novel roles of perivascular nerves on neovascularization. *Neurol Sci*. 2015;36:353–360. doi: 10.1007/s10072-014-2016-x.
29. Kandzari DE, Bhatt DL, Brar S, et al. Predictors of blood pressure response in the SYMPLICITY HTN-3 trial. *Eur Heart J*. 2015;36:219–227. doi: 10.1093/eurheartj/ehu441.
30. Santiago FE, Fior-Chadi DR, Carrettiero DC. Alpha2-adrenoceptor and adenosine A1 receptor within the nucleus tractus solitarii in hypertension development. *Auton Neurosci*. 2015;187:36–44. doi: 10.1016/j.autneu.2014.11.002.
31. Felder RB. Excitatory and inhibitory interactions among renal a cardiovascular afferent nerves in dorsomedial medulla. *Am J Physiol*. 1986:250:580–588.
32. El-Mas MM, Abdel-Rahman AA. Aortic barodenervation up-regulates alpha2-adrenoceptors in the nucleus tractus solitarius and rostral ventrolateral medulla: an autoradiographic study. *Neuroscience*. 1997;79:581–590.
33. De Jong W. Noradrenaline: central inhibitory control of blood pressure and heart rate. *Eur J Pharmacol*. 1974;29:179–181.
34. Totola LT, Alves TB, Takakura AC, Ferreira-Neto HC, Antunes VR, Menani JV, Colombari E, Moreira TS. Commissural nucleus of the solitary tract regulates the antihypertensive effects elicited by moxonidine. *Neuroscience*. 2013;250:80–91. doi: 10.1016/j.neuroscience.2013.06.065.
35. Li D, Wang Q, Zhang Y, Li D, Yang D, Wei S, Su L, Ye T, Zheng X, Peng K, Zhang L, Zhang Y, Yang Y, Ma S. A novel swine model of spontaneous hypertension with sympathetic hyperactivity responds well to renal denervation. *Am J Hypertens*. 2016;29:63–72. doi: 10.1093/ajh/hpv066.
36. Mahfoud F, Moon LB, Pipenhagen CA, Jensen JA, Pathak A, Papademetriou V, Ewen S, Linz D, Böhm M. Catheter-based radio-frequency renal nerve denervation lowers blood pressure in obese hypertensive swine model. *J Hypertens*. 2016;34:1854–1862. doi: 10.1097/HJH.0000000000001021.
37. Stenmark KR, Yeager ME, El Kasmi KC, Nozik-Grayck E, Gerasimovskaya EV, Li M, Riddle SR, Frid MG. The adventitia: essential regulator of vascular wall structure and function. *Annu Rev Physiol*. 2013;75:23–47. doi: 10.1146/annurev-physiol-030212-183802.
38. Raizner AE, Chahine RA, Ishimori T, Verani MS, Zacca N, Jamal N, Miller RR, Luchi RJ. Provocation of coronary artery spasm by the cold pressor test. Hemodynamic, arteriographic and quantitative angiographic observations. *Circulation*. 1980;62:925–932.
39. Lee EW, Michalkiewicz M, Kitlinska J, Kalezic I, Switalska H, Yoo P, Sangkharat A, Ji H, Li L, Michalkiewicz T, Ljubisavljevic M, Johansson H, Grant DS, Zukowska Z. Neuropeptide Y induces ischemic angiogenesis and restores function of ischemic skeletal muscles. *J Clin Invest*. 2003;111:1853–1862. doi: 10.1172/JCI16929.
40. Kanazawa K, Suematsu M, Ishida T, Hirata K, Kawashima S, Akita H, Yokoyama M. Disparity between serotonin- and acetylcholine-provoked coronary artery spasm. *Clin Cardiol*. 1997;20:146–152.

Highlights

- The major findings of the present study are that (1) enhanced SNF and VV formation were noted at the edges of DES implantation sites with enhanced coronary vasoconstricting responses, (2) NTS regions in the central nervous system were influenced by the RDN procedure with resultant decrease in BP and reduced activity of plasma renin and muscle sympathetic nerves, (3) RDN attenuated coronary vasomotion abnormalities after DES implantation in pigs in vivo, (4) RDN also attenuated SNF, VV, and inflammation in the coronary adventitia and Rho-kinase activation after DES implantation, and (5) there were significant correlations between morphological changes (eg, SNF, VV, and inflammatory cell infiltration) and functional changes of the coronary artery (eg, hyperconstricting responses).
- These findings suggest that RDN could be a novel therapeutic option for refractory angina through the kidney–brain–heart axis.

ATVB
Arteriosclerosis, Thrombosis, and Vascular Biology
FIRST PROOF ONLY

Downloaded from http://atvb.ahajournals.org/ by guest on August 20, 2017

Arteriosclerosis, Thrombosis, and Vascular Biology

JOURNAL OF THE AMERICAN HEART ASSOCIATION

Downloaded from http://atvb.ahajournals.org/ by guest on August 20, 2017

Renal Denervation Suppresses Coronary Hyperconstricting Responses After Drug-Eluting Stent Implantation in Pigs in Vivo Through the Kidney –Brain–Heart Axis

Hironori Uzuka, Yasuharu Matsumoto, Kensuke Nishimiya, Kazuma Ohyama, Hideaki Suzuki, Hirokazu Amamizu, Susumu Morosawa, Michinori Hirano, Tomohiko Shindo, Yoku Kikuchi, Kiyotaka Hao, Takashi Shiroto, Kenta Ito, Jun Takahashi, Koji Fukuda, Satoshi Miyata, Yoshihito Funaki, Hatsue Ishibashi-Ueda, Satoshi Yasuda and Hiroaki Shimokawa

Arterioscler Thromb Vasc Biol. published online August 17, 2017;
Arteriosclerosis, Thrombosis, and Vascular Biology is published by the American Heart Association, 7272 Greenville Avenue, Dallas, TX 75231
Copyright © 2017 American Heart Association, Inc. All rights reserved.
Print ISSN: 1079-5642. Online ISSN: 1524-4636

The online version of this article, along with updated information and services, is located on the World Wide Web at:
http://atvb.ahajournals.org/content/early/2017/08/17/ATVBAHA.117.309777

Data Supplement (unedited) at:
http://atvb.ahajournals.org/content/suppl/2017/08/16/ATVBAHA.117.309777.DC1

Permissions: Requests for permissions to reproduce figures, tables, or portions of articles originally published in *Arteriosclerosis, Thrombosis, and Vascular Biology* can be obtained via RightsLink, a service of the Copyright Clearance Center, not the Editorial Office. Once the online version of the published article for which permission is being requested is located, click Request Permissions in the middle column of the Web page under Services. Further information about this process is available in the Permissions and Rights Question and Answer document.

Reprints: Information about reprints can be found online at:
http://www.lww.com/reprints

Subscriptions: Information about subscribing to *Arteriosclerosis, Thrombosis, and Vascular Biology* is online at:
http://atvb.ahajournals.org//subscriptions/

Supplemental Material (for online only)

Hironori Uzuka, MD, PhD;[1] Yasuharu Matsumoto, MD, PhD;[1] Kensuke Nishimiya, MD, PhD;[1,2] Kazuma Ohyama, MD;[1] Hideaki Suzuki, MD, PhD;[1,3] Hirokazu Amamizu, MD;[1] Susumu Morosawa, MD;[1] Michinori Hirano, MD, PhD;[1] Tomohiko Shindo, MD, PhD;[1] Yoku Kikuchi, MD, PhD;[1] Kiyotaka Hao, MD, PhD;[1] Takashi Shiroto, MD, PhD;[1] Kenta Ito, MD, PhD;[1] Jun Takahashi, MD, PhD;[1] Koji Fukuda, MD, PhD;[1] Satoshi Miyata, PhD;[1] Yoshihito Funaki, PhD;[4] Hatsue Ishibashi-Ueda, MD, PhD;[5] Satoshi Yasuda, MD, PhD;[6] Hiroaki Shimokawa, MD, PhD.[1]

Department of Cardiovascular Medicine, Tohoku University Graduate School of Medicine, Sendai, Japan,[1] Wellman Center for Photomedicine, Massachusetts General Hospital, Boston USA,[2] Division of Brain Sciences, Department of Medicine, Imperial College London, United Kingdom,[3] Cyclotron and Radioisotope Center, Tohoku University, Sendai, Japan,[4] and Departments of Pathology[5] and Cardiovascular Medicine,[6] National Cerebral and Cardiovascular Center, Suita, Japan.

Total word count: 615 words

Address for correspondence:

Hiroaki Shimokawa, MD, PhD.
Professor and Chairman
Department of Cardiovascular Medicine
Tohoku University Graduate School of Medicine
1-1 Seiryo-machi, Aoba-ku
Sendai, Japan 980-8574
(Tel) +81-22-717-7152, (Fax) +81-22-717-7156
(E-mail) shimo@cardio.med.tohoku.ac.jp

Supplemental Figures

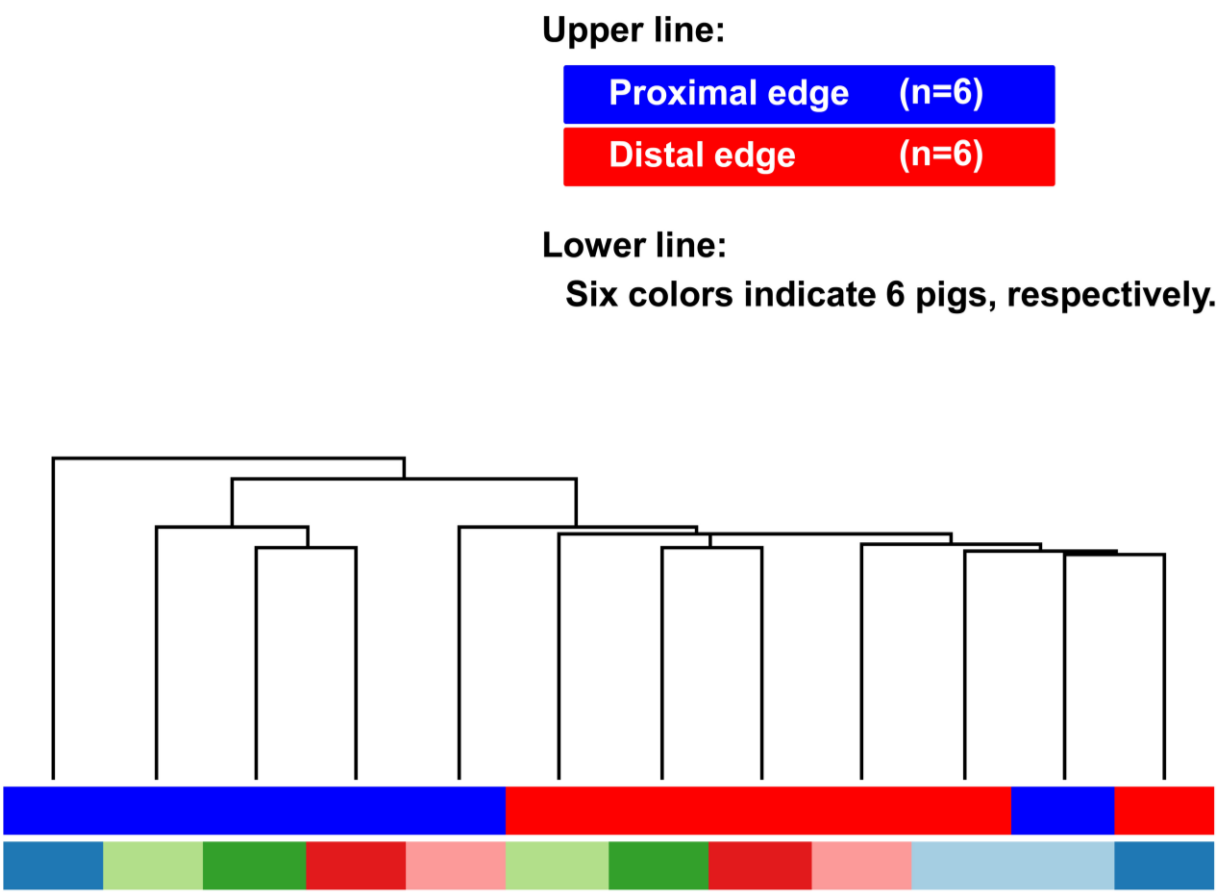

Figure I

Hierarchical clustering with Pearson's correlation as similarity and coefficient and the Ward's clustering in the protocol 1. The number of pigs was 6. Proximal and distal edges in 6 stents (n=6 each) in the protocol 1 were respectively expressed. Apparently, no cluster was detected in this analysis.

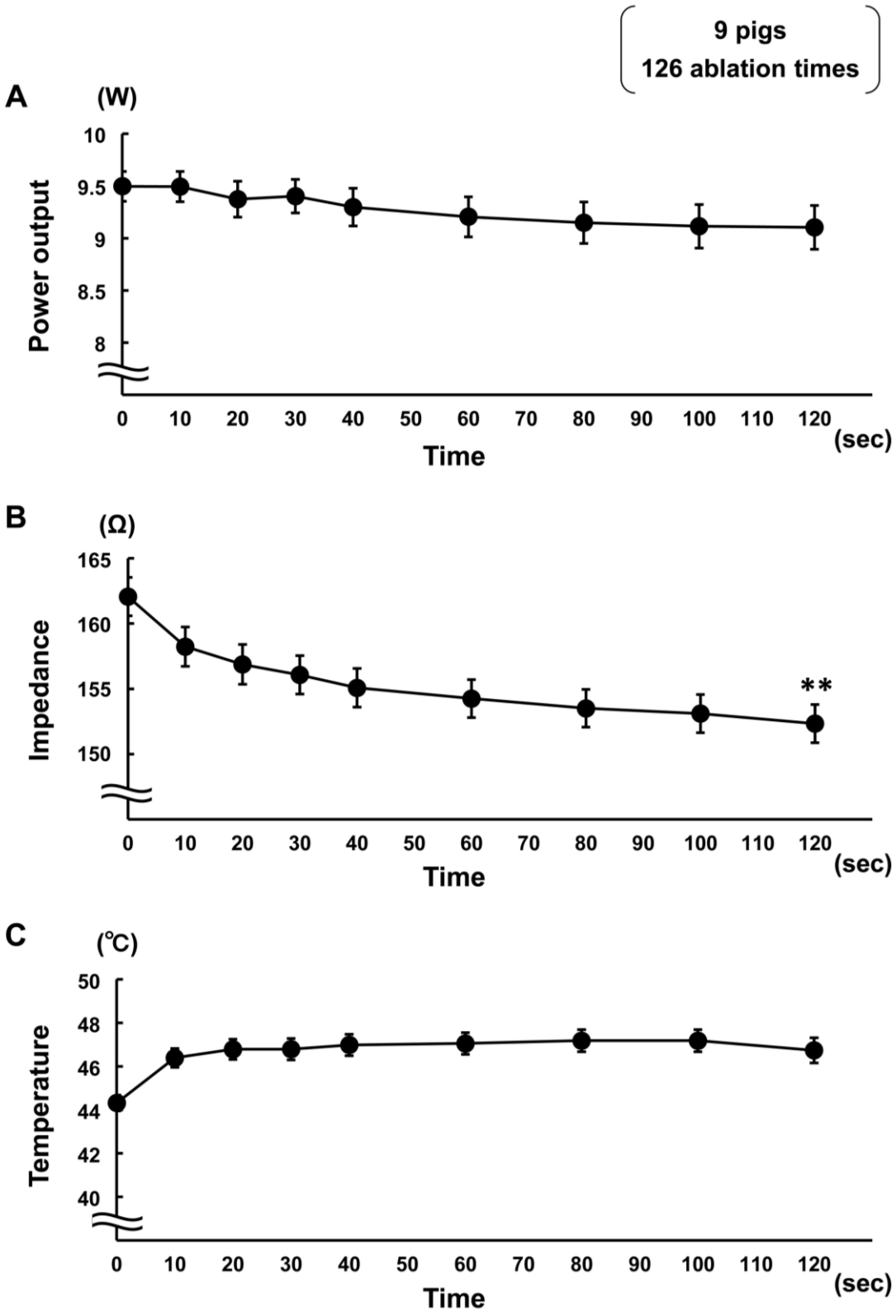

Figure II

Electrophysiological Parameters during Renal Denervation. Changes in power output (**A**), localized impedance (**B**), and localized temperature (**C**) during application. The number of pigs was 9 and the number of ablation times was 126. Results are expressed as mean±SEM. **P<0.01 vs. baseline.

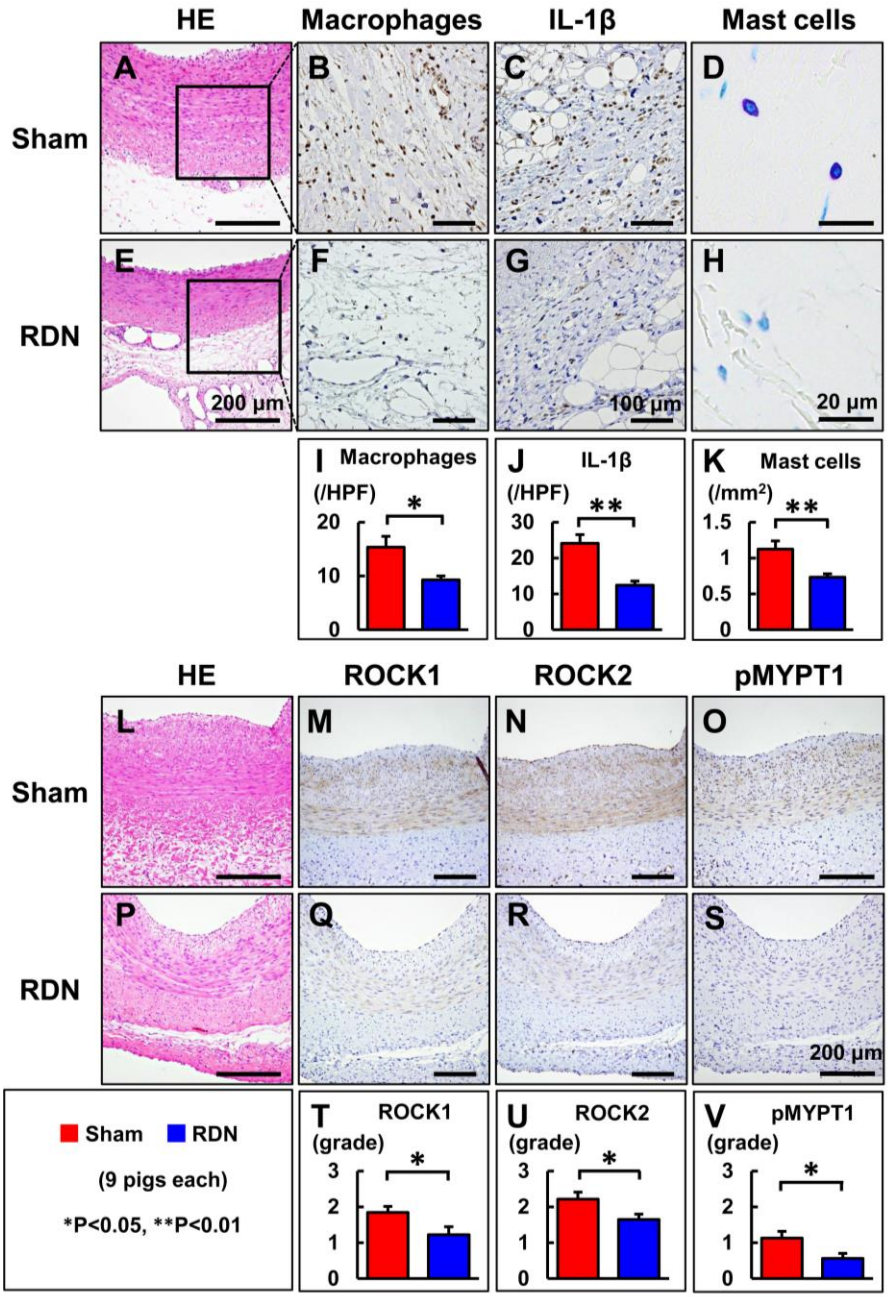

Figure III

Representative pictures at the stent edges for hematoxylin-eosin (HE) stainings (**A, E, L, P**), toluidine blue stainings for mast cells (**D, H**), immunostainings for macrophages (CD68-positive) (**B, F**), interleukin (IL)-1β (**C, G**), ROCK1 (Rho-kinase β) (**M, Q**), ROCK2 (Rho-kinase α) (**N, R**) and phosphorylated myosin phosphatase target subunit-1 (pMYPT1) (a marker of Rho-kinase activation) (**O, S**). Quantitative analysis of cell number in the adventitia for macrophages (**I**), IL-1β-positive cells (**J**) and mast cells (**K**). Semi-quantitative analysis for the extent of ROCK1 (**T**), ROCK2 (**U**) and pMYPT1 (**V**). Scale bars represent 200μm (**A, E, L-S**), 100 μm (**B, C, F, G**) and 20 μm (**D, H**). The number of pigs was 9 each (both Sham and RDN). Results are expressed as mean±SEM. **P<0.01 Sham vs. RDN.

Supplemental Figure Legends

Figure I

Hierarchical clustering with Pearson's correlation as similarity and coefficient and the Ward's clustering in the protocol 1. The number of pigs was 6. Proximal and distal edges in 6 stents (n=6 each) in the protocol 1 were respectively expressed. Apparently, no cluster was detected in this analysis.

Figure II

Electrophysiological Parameters during Renal Denervation. Changes in power output (**A**), localized impedance (**B**), and localized temperature (**C**) during application. The number of pigs was 9 and the number of ablation times was 126. Results are expressed as mean±SEM. **P<0.01 vs. baseline.

Figure III

Representative pictures at the stent edges for hematoxylin-eosin (HE) stainings (**A, E, L, P**), toluidine blue stainings for mast cells (**D, H**), immunostainings for macrophages (CD68-positive) (**B, F**), interleukin (IL)-1β (**C, G**), ROCK1 (Rho-kinase β) (**M, Q**), ROCK2 (Rho-kinase α) (**N, R**) and phosphorylated myosin phosphatase target subunit-1 (pMYPT1) (a marker of Rho-kinase activation) (**O, S**). Quantitative analysis of cell number in the adventitia for macrophages (**I**), IL-1β-positive cells (**J**) and mast cells (**K**). Semi-quantitative analysis for the extent of ROCK1 (**T**), ROCK2 (**U**) and pMYPT1 (**V**). Scale bars represent 200μm (**A, E, L-S**), 100 μm (**B, C, F, G**) and 20 μm (**D, H**). The number of pigs was 9 each (both Sham and RDN). Results are expressed as mean±SEM. **P<0.01 Sham vs. RDN.

Materials and Methods (for online only)

Hironori Uzuka, MD, PhD;[1] Yasuharu Matsumoto, MD, PhD;[1] Kensuke Nishimiya, MD, PhD;[1,2] Kazuma Ohyama, MD;[1] Hideaki Suzuki, MD, PhD;[1,3] Hirokazu Amamizu, MD;[1] Susumu Morosawa, MD;[1] Michinori Hirano, MD, PhD;[1] Tomohiko Shindo, MD, PhD;[1] Yoku Kikuchi, MD, PhD;[1] Kiyotaka Hao, MD, PhD;[1] Takashi Shiroto, MD, PhD;[1] Kenta Ito, MD, PhD;[1] Jun Takahashi, MD, PhD;[1] Koji Fukuda, MD, PhD;[1] Satoshi Miyata, PhD;[1] Yoshihito Funaki, PhD;[4] Hatsue Ishibashi-Ueda, MD, PhD;[5] Satoshi Yasuda, MD, PhD;[6] Hiroaki Shimokawa, MD, PhD.[1]

Department of Cardiovascular Medicine, Tohoku University Graduate School of Medicine, Sendai, Japan,[1] Wellman Center for Photomedicine, Massachusetts General Hospital, Boston USA,[2] Division of Brain Sciences, Department of Medicine, Imperial College London, United Kingdom,[3] Cyclotron and Radioisotope Center, Tohoku University, Sendai, Japan,[4] and Departments of Pathology[5] and Cardiovascular Medicine,[6] National Cerebral and Cardiovascular Center, Suita, Japan.

Total word count: 2,990 words

Address for correspondence:

Hiroaki Shimokawa, MD, PhD.
Professor and Chairman
Department of Cardiovascular Medicine
Tohoku University Graduate School of Medicine
1-1 Seiryo-machi, Aoba-ku
Sendai, Japan 980-8574
(Tel) +81-22-717-7152, (Fax) +81-22-717-7156
(E-mail) shimo@cardio.med.tohoku.ac.jp

Detailed Materials and Methods

All animal care and experiments were performed in accordance with the Guide for the Care and Use of Laboratory Animals published by the U.S. National Institute of Health (NIH Publication, 8th Edition, 2011), and were approved by the Institutional Committee for Use of Laboratory Animals of Tohoku University (2015MdA-067).

We conducted 2 experimental protocols. In the protocol 1 (**Figure 1A**), we examined whether Drug-eluting stents (DES)-induced coronary hyperconstricting responses are associated with enhanced coronary adventitial sympathetic nerve fibers (SNF) formation. In the protocol 2 (**Figure 1B**), we examined whether catheter-based renal denervation (RDN) affects sympathetic autonomic nervous system and whether RDN suppresses coronary hyperconstricting responses after DES implantation in pigs in vivo.

Protocol 1

Male pigs (weighing 25 to 30 kg, N=6) were pre-treated with aspirin (200 mg/day, per os (PO)) and clopidogrel (225 mg/day, PO) for 2 days before stent implantation (**Figure 1A**). After sedation with medetomidine (0.1 mg/kg, intramuscular injection (IM)) and midazolam (0.2 mg/kg, IM), followed by inhaled sevoflurane (2~5%) and heparinization (5,000 U, intravenous injection (IV)), each animal received percutaneous coronary intervention with an everolimus-eluting stent into the left anterior descending coronary artery (LAD) or the left circumflex coronary artery (LCX) randomly (N=6 each). The untreated coronary artery was used as a control artery. To avoid the influence of major side branches (e.g. diagonal and posterolateral branches) on the precise measurement of quantitative coronary angiography (QCA), the stents were deployed across those branches. Balloon inflation ratio was adjusted to achieve an overstretch ratio of 1.0~1.1 under the guidance of intravascular ultrasound (View IT, Terumo Corporation, Tokyo, Japan).[1-4] The dual anti-platelet therapy with aspirin (100 mg/day, PO) and clopidogrel (75 mg/day, PO) was continued until euthanasia. At 1 month after stent implantation, we performed coronary angiography (CAG) to examine coronary vasomotion. After CAG study, the animals were euthanized with a lethal dose of potassium chloride (0.25 mEq/kg, IV) under deep sedation with inhaled 5% sevoflurane. The heart was removed and prepared for histological analysis for coronary adventitial SNF and vasa vasorum .

Protocol 2

Male pigs (N=18) were pre-treated with aspirin (200 mg/day, PO) and clopidogrel (225 mg/day,

PO) for 2 days before stent implantation (**Figure 1B**). After sedation with medetomidine and midazolam, followed by inhaled sevoflurane and heparinization, arterial blood pressure and heart rate were continuously recorded and arterial blood samples were withdrawn. Each animal received percutaneous coronary intervention with everolimus-eluting stents into the LAD and the LCX. After the DES implantation, pigs were randomly assigned to either RDN or sham group (N=9 each). The anti-platelet therapy with aspirin (100 mg/day, PO) and clopidogrel (75 mg/day, PO) was continued until euthanasia. At 1 month after the procedure, blood pressure and heart rate were again recorded and arterial blood samples were withdrawn. We also performed microneurography to evaluate the muscle sympathetic nerve activity.[5] We subsequently performed CAG and renal artery angiography to examine coronary vasomotion and patency of renal arteries. After the angiographies, the animals were euthanized with a lethal dose of potassium chloride (0.25 mEq/kg, IV) under deep sedation with inhaled 5% sevoflurane. The abdominal tissue, the brain, and the heart were removed and prepared for histological and autoradiographic analysis.

RDN Procedure

Following the DES implantation, RDN or sham procedure was performed. After renal artery angiography was performed with a 6-French guiding catheter, the radiofrequency probe (an open-irrigated 3.5-mm-tip catheter, Thermocool, Biosence-Webster, Inc., Diamond Bar, CA, USA) was advanced to 7 points for each renal artery and was energized for 120 sec each at 8~10 Watts in the RDN group or 0 Watts in the sham group with an irrigation flow of 20 ml/min and limiting impedance decrease of 10 Ω.[6] During the procedure, electrophysiological parameters, such as power output, localized impedance, and localized temperature were monitored at every 10 or 20 secs. The radiofrequency ablation therapy was applied as 4-quadrants (circumferential) along the bilateral renal arteries from the distal site at the bifurcation to the main trunk.[7] Final angiography was performed to exclude vessel wall dissection and to document vessel patency and kidney perfusion. After 1 month, the animals again underwent renal artery angiography to confirm vessel patency before euthanasia.

Histological Analysis of the Renal Arteries

To examine the effects of RDN on renal SNF, we performed histological analysis of bilateral renal arteries, as previously described.[8] Briefly, a tissue block including the dorsal muscles, aorta, bilateral kidneys, and bilateral renal arteries was removed as one block and was set into a surface to ensure tissue fixation and structural integrity. The whole tissue was immersed in 10% neutral buffered formalin for at least 24 hours. After fixation, the aorta was dissected to expose the renal ostia. The renal artery and approximately 1.5~2 cm of the

surrounding retroperitoneal connective tissues were isolated and sampled sequentially from the ostium to the hilus approximately every 3 mm. Three samples per renal artery, which were located at proximal, mid and distal sites, were chosen for serially cutting at 3~5 μm and used for Masson's trichrome staining and immunohistochemistry of SNF using rabbit anti-tyrosine hydroxylase (TH) (pSer40) antibody (1:200) (AHP912, AbD Serotec, North Carolina, USA). Percentage of renal nerves affected by the RDN procedure was evaluated by the degree of TH staining intensity in the renal nerves (0=negative, fully damaged; 1=weak (blush), highly damaged; 2=mild, mildly damaged; 3=moderate, almost no changed; and 4=strong, no changed).[9] Furthermore, Grades 0 to 2 were defined as affected nerves and Grade 3 and 4 were defined as not affected. In a total of 54 slides (bilateral proximal, mid, and distal parts of renal arteries in 9 pigs), every renal nerve observed was examined. Moreover, one pig received RDN procedure and euthanized 2 hour later for the assessment of acute effect of RDN on variability of the endothelium of the renal arteries using 1,3,5-triphenyl tetrazolium chloride staining.

Autoradiography of the Brainstem

To examine the brain target of RDN, we performed in vitro autoradiography, as previously described.[10,11] Briefly, the whole brain was removed and immersed in 10% neutral buffered formalin for at least 24 hours. After fixation, under the guidance of an atlas of the pig brain,[12] 5-mm thick coronal sections for the nucleus tractus solitarius were chosen for this study. Sections were cut at 10-μm thick at -20 °C and stored at -80 °C until use. For autoradiographic analysis, the sections were kept at room temperature for 1 hour and then preincubated for 30 min at room temperature in 50 mmol/L Tris HCl (pH 7.4) containing 10 mmol/L $MgCl_2$ and 0.1 μmol/L imipramine in glass Coplin jars to remove endogenous catecholamines.[10] Subsequently, sections were incubated for 60 min at room temperature in Tris-HCl (pH 7.4) containing [^{3}H]rauwolscine, which is a specific radioligand for α_2-adrenergic receptor binding sites (32.0 nmol/L, 2.9 TBq/mmol) (NET722, PerkinElmer, Waltham, Massachusetts), 10 mmol/L $MgCl_2$, 10 nmol/L imipramine, 10 μmol/L pargyline, 0.01% ascorbic acid, and 0.3 μmol/L 5-hydroxytryptamine, which was added to prevent the binding of [^{3}H]rauwolscine to 5-hydroxytryptamine-1A receptors. Non-specific binding of [^{3}H]rauwolscine was measured in the presence of 5 μmol/L (-)-epinephrine. Following intubation, sections were washed three times in ice-cold buffer for 5 min each and then dipped in ice-cold distilled water briefly. The tissue sections were rapidly dried using a stream of cool air and opposed to a tritium-sensitive imaging plates (BAS IP TR 2025 E, Fuji Photo Film, Tokyo) for 72 hours. At the end of the exposure period, autoradiographic images were obtained using an imaging plate system (Fujix Bio-Imaging Analyzer BAS5000, Fuji Photo

Film).[11] Guided by the atlas,[12] a region of interest (ROI) was set at the nucleus tractus solitarius region. The bindings of [^{3}H]rauwolscine was estimated by the photo-stimulated luminescence (PSL) within the ROI. The amount of the binding of [^{3}H]rauwolscine was expressed as the PSL divided by the ROI area.[12]

Microneurography for Sympathetic Nerve Activity

At 1 month after the RDN or sham procedure, we performed microneurography to evaluate the muscle sympathetic nerve activity in pigs in vivo.[5] After exposure of the femoral nerve trunk with skin incision at inguinal area, a fine tungsten microelectrode (model UJ-100-0.2-5.0, about 5 MΩ, Unique Medical Inc., Tokyo, Japan) was gently and carefully inserted into the femoral nerve several times by manual operation until a “spontaneous, intermittent burst” signal, which is one of the general characteristics of the peripheral sympathetic nerve signal, was noted.[5] The original microneurographic signal was filtered (0.5~5 kHz band-pass filter constructed with model UA-200, Unique Medical) and digitally stored (PL3516, PoweraLab16/35, ADInstruments, Australia). The original signal was integrated to assess muscle sympathetic nerve activity with LabChart7 (ADInstruments). The extent of muscle sympathetic nerve activity level was expressed as the number of bursts per minute.[5]

Blood Pressure and Blood Analysis

Arterial blood pressure and heart rate were recorded and arterial blood samples were withdrawn from the femoral artery sheath before RDN or sham procedure and at 1 month after the procedure (**Figure 1B**). Serum levels of sodium, potassium, chloride, blood urea nitrogen and serum creatinine were measured (BML Inc., Tokyo, Japan). Plasma renin activity and plasma levels of aldosterone were also measured (BML Inc.).

In Vivo Assessment of Coronary Vasomotion after DES Implantation

At 1month after DES implantation, we performed CAG to examine coronary vasomotion in pigs in vivo. After control CAG, we examined coronary vasoconstricting responses to serotonin (10 and 100 μg/kg, IC) were examined before and after hydroxyfasudil (30 and 100 μg/kg, IC, for 3 min), a specific Rho-kinase inhibitor (Asahi Kasei Pharma, Tokyo, Japan).[4,13] Coronary vasodilating responses to nitroglycerin (10 μg/kg, IC) and bradykinin (0.1 μg/kg, IC) before and after NG-monomethyl-L-arginine (1 mg/kg, IC for 10 min) were examined. QCA (INFX-8000V, Toshiba Medical Co., Tokyo, Japan) was performed in a blind manner at the proximal and distal edge segments adjacent to the stent as previously described.[1-3] Potential errors for QCA analysis may have occurred. Nevertheless, in 10 randomly selected CAG frames, we examined the accuracy of our QCA analysis as previously described.[14,15] The

interobserver and intraobserver variability for the measurement of QCA in the present study was 4.3±0.9% and 2.7±0.7%, respectively, confirming an acceptable reproducibility and validates the results of our QCA analysis.

Histological Analysis of the Coronary Arteries

The removed heart was prepared for histological analysis (**Figure 1A, B**). For fixation of the coronary arteries, saline and 10% neutral buffered formalin were infused into the left coronary arteries via a constant perfusion pressure system (120 cm H_2O).[1,2,4] After the fixation, the stented coronary artery and the non-stented control artery were isolated for histological analysis. The vessels were separated into the proximal and distal stent edges for paraffin sections with 3~5 μm thickness. The paraffin sections were stained with Masson's trichrome staining. Immunohistochemical staining was performed by using rabbit anti-human von Willebrand factor antibody (1:3) (N1505; Dako, Copenhagen, Denmark) for vasa vasorum and rabbit anti-TH antibody for SNF. The densities of vasa vasorum and SNF were expressed as the number of von Willebrand factor-positive microvessels and TH-positive fibers divided by the adventitial area (/mm^2), respectively. Immunoreactivities for neuropeptide Y and nerve growth factor in SNF were also examined by using rabbit anti- nerve growth factor antibody (1:200) (Ab6199; Abcam) and rabbit anti- neuropeptide Y antibody (1:16,000) (N9528; Sigma, Saint Louis, Missouri). Semi-quantitative analysis regarding the extents of neuropeptide Y and nerve growth factor expressions was evaluated for each TH-positive SNF by using the following scale; 1=slight; 2=moderate; and 3=high.[16]

In the protocol 2, we performed additional histological analysis as shown below (**Figure 1B**). Hematoxylin-eosin, toluidine blue for mast cells, and immunohistochemical stainings were also performed by using mouse anti-CD68 antibody [ED1] (1:50) (Abcam, Cambridge, UK) for macrophages, goat anti-human interleukin-1β (1:50) (AB-201-NA; R&D Systems, Minneapolis, Massachusetts), mouse anti-human Rho-kinase β (ROCK1) antibody (1:50) (61136; BD Biosciences, San Jose, California), mouse anti-Rho-kinase α (ROCK2) antibody (1:50) (610624; BD Biosciences), rabbit anti-human phosphorylated myosin phosphatase target subunit-1 antibody (1:50) (07-251; Millipore, Billerica, Massachusetts), a substrate of Rho-kinase.[1,2,4]

The density of mast cells was expressed as the number of toluidine blue-positive cells divided by the adventitial area (/mm^2). The densities of macrophages and interleukin -β-positive cells were expressed as the number of CD68 and interleukin-β-positive-cells divided by the observation field number (/HPF), respectively.[1,2,4] Semi-quantitative analysis regarding the extent of ROCK1, ROCK2 and phosphorylated myosin phosphatase target subunit-1 was evaluated for each radial subpart per 1 section by using the following scale;

0=none, 1=slight, 2=moderate, and 3=high, as previously described.[2,4,14] Each section was divided into a total 6 radial subparts. For morphometric analysis, each parameter was manually measured by using Image-J (U.S. National Institute of Health, Bethesda, Maryland). Adventitial area was calculated by the following formula; [area outside the external elastic lamina (EEL) within a distance of the thickness of neointima plus media – EEL area].[2,17]

Statistical Analysis

Results are expressed as mean±standard error of mean (SEM) or Tukey boxplots with median values. Throughout the text and figures, N represents the number of pigs, while "n" represents the number of DES edges in the protocol 1, and the number of applications of RDN and renal nerves in the protocol 2. In the protocol 1, we performed hierarchical clustering with Pearson's correlation as similarity coefficient and the Ward clustering method in order to examine the individual difference in the proximal and distal stent edges in a pig. In this analysis, the values of coronary vasoconstricting responses and histological analysis at the edges were used for clustering, and no evident cluster of proximal/distal pairs of same pig was detected (**Figure I in the online-only Data Supplement**). Based on this analysis, various changes at the proximal and distal edges in a pig were treated as individual factors in the protocol 1. In the protocol 2, since RDN is a systemic intervention, we evaluated the values by taking average of four sites at the proximal and distal edges in the LAD and LCX with regard to vasoconstricting/vasodilating responses and histology. A comparison of the QCA and histomorphometry was performed by using an unpaired, 2-sided Student's t-test. Comparison of the semi-quantitative analysis was performed by using a Mann-Whitney U-test. The correlation between the continuous variables was analyzed using a linear regression model. Statistical analysis was performed with IBM SPSS Statistics 20 (IBM, New York, NY, USA). A value of $P<0.05$ was considered to be statistically significant.

Supplemental References

1. Tsuburaya R, Yasuda S, Shiroto T, Ito Y, Gao JY, Aizawa K, Kikuchi Y, Ito K, Takahashi J, Ishibashi-Ueda H, Shimokawa H. Long-term treatment with nifedipine suppresses coronary hyperconstricting responses and inflammatory changes induced by paclitaxel-eluting stent in pigs in vivo: possible involvement of Rho-kinase pathway. Eur Heart J. 2012:33:791-799.
2. Nishimiya K, Matsumoto Y, Shindo T, Hanawa K, Hasebe Y, Tsuburaya R, Shiroto T, Takahashi J, Ito K, Ishibashi-Ueda H, Yasuda S, Shimokawa H. Association of adventitial vasa vasorum and inflammation with coronary hyperconstriction after drug-eluting stent implantation in pigs in vivo. Circ J. 2015:79:1787-1798.
3. Shiroto T, Yasuda S, Tsuburaya R, Ito Y, Takahashi J, Ito K, Ishibashi-Ueda H, Shimokawa H. Role of Rho-kinase in the pathogenesis of coronary hyperconstricting responses induced by drug-eluting stents in pigs in vivo. J Am Coll Cardiol. 2009:54: 2321-2329.
4. Nishimiya K, Matsumoto Y, Uzuka H, Ogata T, Hirano M, Shindo T, Hasebe Y, Tsuburaya R, Shiroto T, Takahashi J, Ito K, Shimokawa H. Beneficial effects of a novel bioabsorbable polymer coating on enhanced coronary vasoconstricting responses after drug-eluting stent implantation in pigs in vivo. J Am Coll Cardiol Intv. 2016:9:281-291.
5. Nakamura T, Kawahara K, Kusunoki M, Feng Z. Microneurography in anesthetized rats for the measurement of sympathetic nerve activity in the sciatic nerve. J Neurosci Methods. 2003:131:35-39.
6. Kiuchi MG, Maia GL, de Queiroz Carreira MA, Kiuchi T, Chen S, Andrea BR, Graciano ML, Lugon JR. Effects of renal denervation with a standard irrigated cardiac ablation catheter on blood pressure and renal function in patients with chronic kidney disease and resistant hypertension. Eur Heart J. 2013:34:2114-2121.
7. Kandzari DE, Bhatt DL, Brar S, et al. Predictors of blood pressure response in the SYMPLICITY HTN-3 trial. Eur Heart J. 2015:36:219-227.
8. Tellez A, Rousselle S, Palmieri T, Rate WR 4th, Wicks J, Degrange A, Hyon CM, Gongora CA, Hart R, Grundy W, Kaluza GL, Granada JF. Renal artery nerve distribution and density in the porcine model: biologic implications for the development of radiofrequency ablation therapies. Trans Res. 2013:162:381-389.
9. Cohen-Mazor M, Mathur P, Stanley JR, Mendelsohn FO, Lee H, Baird R, Zani BG, Markham PM, Rocha-Singh K. Evaluation of renal nerve morphological changes and norepinephrine levels following treatment with novel bipolar radiofrequency delivery

systems in a porcine model. J Hypert. 2014:32:1678-1691; discussion 1691-1692.

10. El-Mas MM, Abdel-Rahman AA. Aortic barodenervation up-regulates alpha2-adrenoceptors in the nucleus tractus solitarius and rostral ventrolateral medulla: an autoradiographic study. Neuroscience. 1997:79:581-590.
11. Funaki Y, Kato M, Iwata R, Sakurai E, Sakurai E, Tashiro M, Ido T, Yanai K. Evaluation of the binding characteristics of [5-(11)C-methoxy]Donepezil in the rat brain for in vivo visualization of acetylcholinesterase. J Pharmaco Sci. 2003:91:105-112.
12. Felix B, Leger ME, Albe-Fessard D, Marcilloux JC, Rampin O, Laplace JP. Stereotaxic atlas of the pig brain. Brain Res Bull. 1999:49:1-137.
13. Shimokawa H. 2014 Williams Harvey Lecture: importance of coronary vasomotion abnormalities-from bench to bedside. Eur Heart J. 2014:35:3180-3193.
14. Aizawa K, Yasuda S, Takahashi J, Takii T, Kikuchi Y, Tsuburaya R, Ito Y, Ito K, Nakayama M, Takeda M, Shimokawa H. Involvement of Rho-kinase activation in the pathogenesis of coronary hyperconstricting responses induced by drug-eluting stents in patients with coronary artery disease. Circ J. 2012:76:2552-2560.
15. Matsumoto Y, Adams V, Jacob S, Mangner N, Schuler G, Linke A. Regular exercise training prevents aortic valve disease in low-density lipoprotein-receptor-deficient mice. Circulation. 2010:121:759-767.
16. Qin F, Vulapalli RS, Stevens SY, Liang CS. Loss of cardiac sympathetic neurotransmitters in heart failure and NE infusion is associated with reduced NGF. Am J Physiol Heart Circ Physiol. 2002:282:H363-371.
17. Kwon HM, Sangiorgi G, Ritman EL, Lerman A, McKenna C, Virmani R, Edwards WD, Holmes DR, Schwartz RS. Adventitial vasa vasorum in balloon-injured coronary arteries: visualization and quantitation by a microscopic three-dimensional computed tomography technique. J Am Coll Cardiol. 1998:32:2072-2079.